Modification of the petroleum system concept: Origins of alkanes and isoprenoids in crude oils

James Collister, Robert Ehrlich, Frank Mango, and Glenn Johnson

ABSTRACT

Kerogen, the source material for petroleum, can have a long history of alteration and diagenesis before crude oil forms. A common assumption is that the bulk composition of the expressed oil reflects so much of these progressive alterations that most of the primary biological information of the original fixed carbon has been lost. Exceptions are trace constituents, the biomarkers that comprise only a fraction of the organic material in most pristine crude oils. Analysis of the alkane/acyclic isoprenoid fraction of a large number of crude oils and rock extracts from the Timan-Pechora basin (Russia) suggest that this fraction, the main constituent of most crude oils, is a direct product of liquefaction of biological debris that was preserved essentially unaltered to the point of oil generation. Therefore, the primary biological provenance of this fraction is preserved in the oil fraction.

A set of gas-chromatographic analyses of 242 crude oils as well as 83 solvent extracts from upper to middle Paleozoic putative source rocks from the Timan-Pechora basin (Russia) were analyzed by a multivariate data-analytical procedure new to organic geochemistry. The distributions of n-alkanes and acyclic isoprenoids (24 in all) in the 325 samples could be reproduced by linear combinations of six end-member compositions attributed to distinct biological inputs. Four of the six are assigned to primary producers (waxes from higher plants, cyanobacteria, microalgae, and the microorganism *Gloeocapsomorpha prisca*). These end members account for most of the n-alkanes and acyclic isoprenoids in our samples. The other two represent the products of secondary bacterial alteration of primary organics during sedimentation and low-level bacterial alteration in the reservoir (biodegradation). Each end member is composed of a spectrum of analytes whose abundances are related to one another by fixed ratios. We surmise that each primary end member represents

Manuscript received March 3, 2003; provisional acceptance August 22, 2003; revised manuscript received December 3, 2003; final acceptance January 7, 2004.

DOI:10.1306/01070403019

AUTHORS

JAMES COLLISTER ~ *SGS Control Services, 22934 Lochness Ave., Torrance, California 90105; James_Collister@sgs.com*

James Collister received a B.A. degree in biochemistry and geology from the University of California at Santa Barbara and an M.S. degree and a Ph.D. in biogoechemistry from Indiana University. He is currently working at SGS Control Services in California and is also a private consultant. His interests include isotopic biogeochemistry of ancient and modern sedimentary depositional environments, oil and source rock characterization, and tracing biogenic inputs into petroleum source rocks and crude oils in an attempt to refine petroleum systems analysis.

ROBERT EHRLICH ~ *Residuum Energy, Inc., 1048 S. Oak Hills Way, Salt Lake City, Utah 84108; bobehrlich@residuumenergy.com*

For the past 30 years, Robert Ehrlich has been engaged in developing and applying image analysis and pattern recognition procedures in the earth and environmental sciences. He received his B.A. degree in geology at the University of Minnesota. He received his M.S. degree and his Ph.D. from Louisiana State University. After a 30-year career in the academe at Michigan State University, the University of South Carolina, and the University of Utah, he is currently vice president of Residuum Energy Incorporated and heads Residuum's Salt Lake City office. He current interests lie in the general field of data mining.

FRANK MANGO ~ *Department of Chemical Engineering, Rice University, PO Box 1892, Houston, Texas 77079-5201; fmango@houston.rr.com*

Frank Mango received his B.S. degree in chemistry from San Jose State College and his Ph.D. in organic chemistry from Stanford University. He joined Shell Development at Emeryville, California, working in catalysis and petroleum chemistry and later switched to organic geochemistry at Bellaire Research Center in Texas. He was adjunct professor in the Department of Geology and Geophysics at Rice University and a research scientist in the Department of Chemical Engineering, where he carried out research on the role of transition metals in the origin of oil and natural gas.

GLENN JOHNSON ~ *University of Utah, Energy and Geoscience Institute, 423 Wakara Way, Suite 300, Salt Lake City, Utah 84108; gjohnson@egi.utah.edu*

Glenn Johnson received his M.S. degree from the University of Delaware and his Ph.D. from the University of South Carolina. Both research programs focused on the application of multivariate techniques to geological and geochemical data. He spent seven years between degrees, as an environmental consultant with Roux Associates, Inc., and McLaren/Hart Environmental Engineering Corp., where his work focused on investigation of contaminated sites, environmental forensics, and associated litigation support. Since 1995, Johnson has been a research assistant professor at the Energy and Geoscience Institute at the University of Utah, where he teaches in the Department of Civil and Environmental Engineering, and continues research in chemometrics applied to environmental and petroleum geochemical systems.

ACKNOWLEDGEMENTS

The Timan-Pechora oils and rock extracts were analyzed in the laboratory of the Energy and Geoscience Institute, University of Utah. The high quality of the analyses owes much to the care and prowess of Nicolas Dahdah.

the breakdown of a resistant biopolymer that forms cell walls and partitions of a given biological group. The n-alkanes and acyclic isoprenoids in crude oils represent the weighted signatures of their various ancestors (i.e., their primary organic inputs). If the precursors of most oils are the products of a small set of chemically simple biopolymers, then many of our assumptions concerning the importance of total organic carbon and the nature of the oil window must be reexamined.

INTRODUCTION

Assessment of new plays includes an aspect associated with the existence and maturity of significant amounts of fossil organic matter, as well as factors that control the timing of expulsion of hydrocarbons. All of this depends on the composition and stability of tiny particles of fossil organic matter that in aggregate is termed ''kerogen.'' Therefore, any modification of our ideas with respect to the manner in which kerogen is converted to petroleum will modify our understanding of the petroleum system. Most of the effort in the past has concentrated on microscopic observations of kerogen and laboratory experiments that model the conversion of kerogen to petroleum. In this paper, we come from another direction. Based on the compositional variation among a large suite of related oil samples, we infer the origins of an important and valuable fraction of crude oil. These observations, in conjunction with laboratory studies of source rock, raise the possibility of a major change in our thinking about an important part of the petroleum system. The issue revolves around the extent that this material retains its primary chemistry (a chemical fingerprint) all through the stages of maturation from diagenesis to conversion to petroleum.

There is general agreement that compositional variations in crude oils reflect both differences between biological precursors of kerogen as well as the processes responsible for the conversion of kerogen to oil and gas (catagenesis). However, there is no consensus on the relative contributions of these two sources of variability to the composition of crude oils. In other words, the degree of preservation of the initial imprint of the primary organic provenance remains an open question. Although a group of trace constituents, the biomarkers, remain remarkably unchanged in sedimentary basins and thus provide some information on provenance (for examples, see Peters and Moldowan, 1993), the dominant hydrocarbons in crude oils, the n-alkanes and acyclic isoprenoids, are not currently viewed as particularly diagnostic in this regard. They may or may not contain the fingerprints of their biological ancestors. Our objective here is to establish the diagnostic importance of the C_{10} to C_{28} n-alkane and acyclic isoprenoids.

A biological fingerprint requires the preservation of a carbon skeleton traceable to a specific organism (Mackenzie et al., 1982). However, carbon skeletons may suffer microbial alteration during sedimentation and early burial (early diagenesis) or may be altered

in the destructive processes associated with oil generation and kerogen maturation. Amorphous kerogen is, by and large, the product of highly modified (largely by bacteria) organic detritus that then reacted to form kerogen. This process has been termed the ''degradation-recondensation pathway'' for kerogen formation (de Leeuw and Largeau, 1993). One might expect minimal preservation of a primary organic structure in such material excepting trace constituents such as biomarkers.

However, not all organic detritus need follow this diagenetic pathway. Highly resistant fragments of an organism (e.g., membrane constituents in the form of biopolymers) may be selectively preserved relative to free lipids, amino acids, proteins, and polysaccharides and incorporated into kerogen (Tegelaar et al., 1989). Fragments of cell walls or other protective layers have been optically identified in kerogens (Chalansonnet et al., 1988; Tegelaar et al., 1989; Largeau et al., 1990; Derenne et al., 1991; Gelin et al., 1999). Such selectively preserved biopolymers in kerogen have potential for carrying primary biological information intact to subsequently evolved crude oils (Collister et al., 1992; Eglinton, 1994). Even so, whether the destructive processes that produce petroleum also destroy evidence of these biological signals preserved in kerogen up to that point is in question. In addition, if they survive, do these biologically derived lipids constitute a significant fraction of expelled oil? Our analysis indicates yes, the n-alkanes and acyclic isoprenoids in the C_{10} to C_{28} fraction of petroleum, the largest reservoir of hydrocarbons in most oils, retain substantial information on primary organic provenance.

THE N-ALKANE/ACYCLIC ISOPRENOID FRACTION OF CRUDE OIL

A particular combination of the 24 n-alkanes and acyclic isoprenoids between C_{10} and C_{28} in a sample is henceforth referred to as a sample ''spectrum.'' Consideration of the entire spectrum is necessary in that the individual n-alkanes and acyclic isoprenoids between C_{10} and C_{28} can be produced by several processes and from a variety of biological precursors, and so there is no single compound in this fraction that is diagnostic of a specific source. However, it is possible that different sources produce different distributions of these hydrocarbons (i.e., different spectra). If so, then this oil fraction could contain the fingerprints of biological precursors, provided these spectra survive the destructive processes of oil generation and maturation.

The Concept of End-Member Fingerprints

We assume that the composition of a given crude oil has several biological and process inputs and so consists of a mixture of diagnostic spectra. A crude oil can be a mixture for a variety of other reasons, including the obvious ones: multiple migration pathways or multiple source rocks feeding oil into a single reservoir. Even within a single source rock, kerogen that is a variable mixture of various biological sources may generate oil that is a mixture of simpler spectra, each of which represents the contribution of a kerogen type. Alternatively, given a source rock containing only one kerogen type, several different spectra may be generated over time as temperature increases. We might, for instance, find that oils generated at high temperatures might contain fewer long-chained hydrocarbons than those generated at low temperatures.

If such primary spectra (from process or biology) are known beforehand, they would constitute a library of source fingerprints. Given such a library, it would be mathematically straightforward to numerically ''unmix'' any oil into the linear combination of the primary spectra that best define it. Unfortunately, no such library currently exists, and at our current state of knowledge, we can either define them from a purely theoretical viewpoint or derive them from analysis of the chemistry of samples of crude oils.

Derivation of Primary Spectra (End Members) Solely from a Suite of Oils

There is, however, a statistical method that essentially deconvolves a large database of spectra into a finite number of end-member spectra using only the sample spectra as raw material. No prior assumptions need be made in terms of the number of spectra present in the data set or the composition of each spectrum. The procedure, polytopic vector analysis, extracts end-member spectra from mixed systems (Full et al., 1982), and it does not require a preexisting library of end-member spectra. Instead, polytopic vector analysis yields the library from the sample data, giving (1) the spectrum of each end member and (2) the proportion of each end member in each sample of the database. A complete description (and literature review) of polytopic vector analysis in the context of mixed organic systems can be found in Johnson et al. (2002).

A polytope is a geometrical figure that represents the generalization of a polygon in two dimensions and a polyhedron in three dimensions to any number of

dimensions. Note that a polytope has one vertex more than the number of dimensions in which it is embedded. Whenever we plot data on a ternary diagram, we are plotting the sample vectors onto a triangle (a two-dimensional polytope) whose three vertices represent end members.

Each sample is composed of k compounds and so is a vector with k elements. If the compositions are reported as relative proportions of k compounds, a polytope embedded in k-1 dimensions can always enclose a collection of such data vectors. However, the laws of chemistry ensure that the compounds are, to a large extent, mutually correlated. This reduces the dimensionality of the polytope. Polytopic vector analysis contains two modules. The first module attempts to determine via principal component analysis the minimum number of dimensions that will contain the data vectors without distortion. For instance, the plagioclase feldspars consist of four cations (K, Na, Al, and Si), and so one might suppose that four dimensions (each dimension containing an axis measuring the variation of a single cation) would be necessary in which to embed the plagioclase polytope. The four vertices of such a tetrahedron represent end-member compositions that enclose the sample vectors. However, analysis of the plagioclase data set using the criteria in the first module would show that only one dimension is necessary, a polytope represented by a one-dimensional, two–end-member line. That is, all of the plagioclases can be considered mixtures of two end members, albite and anorthite. Hence, in the sense of classification space, the plagioclases are a one-dimensional system, and considered in that way, no information is lost if all plagioclases are considered to be mixtures of albite and anorthite. In the case of our samples, the procedure suggested a five–end-member solution (see Johnson et al., 2002, for details).

Given the determination of the true dimensionality of classification space, the second module in polytopic vector analysis iteratively constructs a polytope wherein all of the sample vectors are on or in it (no negative mixing proportions), and the composition of every vertex contains no negative values. The only fundamental assumption is that each end member must be in very small abundance in at least one sample in the sample set.

This procedure does not always converge (it sometimes diverges), indicating that sometimes, not enough information is present in the set of sample vectors to construct a valid polytope, or that the data set contains major errors.

In the case of the alkane/isoprenoid data vectors in this investigation, a six–end-member solution converged, and so, all sample spectra in the data set can be considered mixtures of six end members (all samples fit on or in the polytope). Each end member is represented by the composition at one of the six vertices.

ANALYTICAL PROCEDURES

We initially examined the alkanes and isoprenoids compositions of 142 crude oils and 83 rock extracts from the Timan-Pechora basin in Russia (Appendices 1, 2). Crude oils biodegraded beyond rank 3 (Peters and Moldowan, 1993), and extracts of severely weathered rock samples were excluded from this database. We analyzed three data matrices generated by the gas chromatography–flame ionization detection (GC-FID) analysis: one for Timan-Pechora crude oils, another for potential source rock extracts, and a third where the two sets were combined.

Organic-rich Devonian marine shales containing type II kerogens are believed to be the major source of hydrocarbons in this petroleum system (Ulmischek, 1982; Requejo et al., 1995; Tull, 1997; Abrams et al., 1999). Because they occupy a variety of positions in the oil window, large variations in oil maturity are anticipated in this basin (Ulmischek, 1982; Abrams et al., 1999). Therefore, in the absence of multiple biological sources, variations between samples would reflect the effects of progressive expulsion under various time and temperature scenarios and the effects of secondary alteration (e.g., biodegradation, water washing).

Hydrocarbons were solvent extracted from a small, pulverized sample of a putative source rock. These extracts represent weakly bound fractions that are probably not incorporated into the extant kerogen. Instead, they represent fractions that have been produced in the source rock but not expelled.

A total of 779 rock samples and 158 crude oils from the Timan-Pechora basin (Russia) were available for analysis. The rock samples were screened for source potential with a pyrolysis method that established the total organic carbon (TOC) content during the Rock-Eval pyrolysis (Delsi Instruments, Rock-Eval II; performed by Humble Instruments and Services). Rock samples suspected of being stained with nonindigenous hydrocarbons were not chosen for soxhlet extraction and subsequent GC-FID analysis. These include samples with a production index $[S_1/(S_1 + S_2)]$ greater than 0.4 or a total generation potential $(S_1 + S_2)$ that is disproportionately high relative to the TOC content. Total generation potentials $(S_1 + S_2)$ increased as a

function of roughly six times TOC contents for the majority of the rocks. Rocks significantly above this trend (i.e., elevated TGPs [total generation potential calculated from Rock-Eval output]) were not extracted. One hundred thirty-six rock samples were chosen for soxhlet extraction and subsequent GC-FID analysis (Appendices 1, 2). Rock samples (about 40–60 g) were powdered to −10-μm mesh, loaded into coarse alundum thimbles, and soxhlet extracted with dichloromethane for 16–24 hr. The condensers were connected in series to a Brinkman® water circulator that was set to 10°C. After extraction, excess solvent was removed by rotary evaporation, and residual solvent was removed under a stream of nitrogen.

Whole bitumen extracts and whole (untopped) crude oils were analyzed for n-alkanes and acyclic isoprenoids using a Hewlett Packard 5890 gas chromatograph equipped with a flame ionization detector. Split injection (50:1) was employed at 300°C (detector temperature = 350°C) onto a nonpolar Restek® column (30 m × 25 mm × 0.25 μm; Rtx-1). Helium was used as the carrier gas, and the GC column temperature was programmed from 35°C (2 min isothermal) to 310°C at 4°C/min (29.25 min isothermal). Autosamplers were used to increase efficiency and achieve reproducible injections. Data were collected and processed with Minichrom software from VG Analytical. Integrated peak heights for GC-FID data from n-C_{10} to n-C_{28} were provided for statistical analysis. Compounds lighter than n-C_{10} were not integrated because of potential loss caused by devolatilization and potential effects of biodegradation and water washing (secondary alteration). Compounds heavier than n-C_{28} were not integrated because of coelution with abundant biomarkers in some samples. Severely biodegraded crude oils (i.e., rank 4 or higher on the Peters and Moldowan, 1993, scale) were excluded from the data analysis. After screening before and after analysis, 227 samples comprising 83 rock extracts and 144 oil samples were used in the statistical analysis.

RESULTS

The oils and rock extracts were initially analyzed (via polytopic vector analysis) as separate data sets. Using goodness-of-fit diagnostics described by Johnson et al. (2002), the same six end members defined both data sets. Goodness of fit was measured by the coefficient of determination (R^2) that indicates how well the composition of each compound could be approximated using a six–end-member solution. The coefficients of determination ranged from 0.88 (n-C_{13}) to 0.98 for most other compounds. The polytopic vector analysis results on the combined sets are shown in Tables 1 and 2. As might be expected, the rock extracts showed the greatest variations in end-member compositions. The exception to the rule involves an end member representing the extract of an unknown microorganism (EM 6). It contributes to only a small number of the rock extracts but is a major contributor to the oils. The greater variability in the crudes permits a more accurate estimate to that end member's overall contribution.

Description of End Members

Five of the six end members can be assigned to specific primary organic inputs: photosynthetic algae/heterotrophic bacteria (end members 5 and 6), cyanobacteria (end member 2), a high wax source (end member 1), and products of the organism *Gloeocapsomorpha prisca* (end members 4). The remaining end member represents an intermediate stage of reservoir biodegradation (end member 3). The chemical compositions of these end members are summarized in Table 1 and Figure 1. These end members suffice for both the rock extracts and the oils.

EM 1 (Wax)

The first end member (EM 1) is attributed to a high wax source, probably from terrestrial higher plants. A unimodal envelope of C_{16} to C_{28} n-alkanes dominates its spectrum, with a maximum at n-C_{25} (Figure 1a), and the acyclic isoprenoids are absent, with the exception of phytane. The strongly convex aspect of the envelope in the long-chain region of the chromatogram (Figures 1a, 2a, 3a, 4) is typical of crude oils generated from source facies containing terrestrial, wax-rich components (Ruble et al., 1994; Peters et al., 2000). Epicuticular leaf waxes display a strong odd-carbon preference commonly observed in the range of n-C_{25} to n-C_{33} (e.g., Collister et al., 1994) This feature is lacking from this end member and is not readily apparent in chromatograms of crude oils and rock extracts high in this end member (Figures 2a, 3a, 4). This suggests that EM 2 represents release of alkanes from a refractory waxy biopolymer associated with higher plants instead of free leaf waxes that were subsequently incorporated into the kerogen. The range of EM 1 proportions is similar in both the rock extracts and the crude oils and ranges from near zero in some samples to as much as 55% in others, averaging 22% (Table 2).

Table 1. End Member Compositions for Crude Oils and Potential Source Rocks (relative proportions of each component)

Compound	EM 1 Waxy	EM 2 Cyanobacteria	EM 3 Biodegradation	EM 4 *G. prisca*	EM 5 Open-Marine	EM 6 Microbial
n-C_{10}	0.00	27.13	0.00	0.00	2.59	0.00
n-C_{11}	0.00	25.61	0.50	1.88	0.00	10.16
n-C_{12}	0.00	17.28	0.00	0.00	0.00	20.24
n-C_{13}	0.00	12.87	0.00	11.63	0.00	15.63
n-C_{14}	0.30	8.60	0.00	8.59	0.00	20.81
i-C_{16}	0.00	0.53	18.66	0.00	4.52	2.66
n-C_{15}	0.00	4.80	1.20	17.02	1.88	14.30
n-C_{16}	0.93	1.91	0.00	14.28	11.47	7.21
i-C_{18}	0.00	0.00	17.29	1.09	2.72	0.00
n-C_{17}	1.81	1.27	0.29	25.14	0.21	4.42
pristane	0.00	0.00	29.05	0.00	4.11	0.00
n-C_{18}	5.32	0.00	0.00	5.04	14.44	3.81
phytane	1.34	0.00	22.44	0.00	0.00	0.00
i-C_{21}	0.00	0.00	4.50	1.53	0.00	0.00
n-C_{19}	5.17	0.00	0.21	11.14	9.88	0.00
n-C_{20}	7.60	0.00	2.53	1.15	13.29	0.73
n-C_{21}	8.60	0.00	1.40	0.33	11.94	0.00
n-C_{22}	9.27	0.00	1.70	0.05	9.09	0.00
n-C_{23}	9.92	0.00	0.00	0.34	6.62	0.00
n-C_{24}	10.28	0.00	0.00	0.14	4.05	0.00
n-C_{25}	10.49	0.00	0.00	0.32	2.36	0.00
n-C_{26}	10.45	0.00	0.23	0.00	0.82	0.00
n-C_{27}	9.86	0.00	0.00	0.33	0.00	0.00
n-C_{28}	8.66	0.00	0.00	0.00	0.00	0.02

Rock extracts containing greater than 20% EM 1 are almost exclusively confined to Middle and Upper Devonian samples. Crudes containing more than 20% occur almost exclusively in Middle and Upper Devonian reservoirs (Table 2). In contrast, low-wax crude oils are concentrated in Lower Devonian and Carboniferous–Triassic reservoirs. EM 1 concentrations are inversely related to EM 2 (cyanobacteria) concentrations in both the rock extracts and the oils. Each reaches its maximum in samples where the other reaches its minimum.

EM 2 (Cyanobacteria)

EM 2 exhibits a unimodal distribution of n-alkanes with an exponential decay, a maximum at n-C_{10} and truncation at n-C_{18} (Figure 1b). The spectrum contains low amounts of the shorter chain acyclic isoprenoids (i-C_{16} and i-C_{18}) and none of the longer chain isoprenoids (e.g., pristane, phytane, and i-C_{21}). Although free lipids from microbial primary producers display a strong odd-carbon preference in the range of n-C_{15} to n-C_{21} (Han et al., 1968, 1980; Han and Calvin, 1969; Jones, 1969; Gelpi et al., 1970), no carbon preference is observed in the end member or in the chromatograms of samples high in this EM (Figures 2b, 3b, 5). Therefore, incorporation of free algal lipids into the kerogen via the condensation pathway is unlikely to account for the fingerprint of this end member. Thermal breakdown of a refractory biopolymer from the cell walls of cyanobacteria probably accounts for the chemical composition of this end member.

Independent chemical evidence supports the interpretation of cyanobacteria as a source for EM 2. The key to recognition of the cyanobacterial biological sources lies in the hydrocarbons not included in this analysis, namely, the monomethyl alkanes, which are a set of minor peaks observed in the gas chromatograms of samples enriched in EM 2. Figure 5a shows the chromatogram of TP405R, which is 49% EM 2. The monomethyl alkanes appear as homologs eluting between the more abundant n-alkanes. These hydrocarbons are a distinguishing characteristic of extracts from cyanobacteria (Han et al., 1968; Gelpi et al., 1970;

Table 2. Mixing Proportions of End Members for Timan-Pechora Rock Extracts and Crude Oils

Sample	Age	EM 1 Waxy	EM 2 Cyanobacteria	EM 3 Biodegradation	EM 4 *G. prisca*	EM 5 Open-Marine	EM 6 Microbial
TP018R	Middle Devonian	0.456	0.101	−0.026	0.176	0.192	0.101
TP042R	Lower Carboniferous	0.203	0.231	0.115	0.130	0.089	0.232
TP084R	Middle(?) Devonian	0.259	0.151	−0.027	0.190	0.230	0.197
TP117R	Upper Devonian	0.385	0.106	0.034	0.211	0.108	0.157
TP123R	Middle Devonian	0.262	0.084	0.017	0.247	0.148	0.243
TP137R	Upper Devonian	0.159	0.283	0.021	0.172	0.154	0.211
TP138R	Upper Devonian	0.228	0.234	0.007	0.178	0.169	0.184
TP141R	Upper Devonian	0.297	0.185	−0.029	0.164	0.222	0.161
TP154R	Upper Devonian*	0.106	0.281	0.126	0.138	0.183	0.166
TP156R	Upper Devonian*	0.149	0.256	0.166	0.160	0.159	0.110
TP169R	Upper Devonian	0.232	0.282	0.023	0.161	0.178	0.122
TP198R	Lower Devonian	0.493	−0.044	0.026	0.247	0.148	0.131
TP209R	Upper Devonian	0.236	0.251	−0.013	0.174	0.181	0.171
TP212R	Upper Devonian	0.296	0.203	0.001	0.169	0.179	0.153
TP242R	Middle Devonian	0.133	0.368	0.002	0.201	0.095	0.200
TP243R	Middle Devonian	0.421	0.102	−0.018	0.187	0.064	0.244
TP247R	Middle Devonian	0.357	0.208	−0.023	0.154	0.129	0.176
TP298R	Upper Silurian	0.227	0.243	0.101	0.172	0.068	0.189
TP299R	Upper Silurian	0.253	0.209	0.143	0.197	0.105	0.094
TP323R	Lower Devonian	0.050	0.262	0.043	0.475	0.023	0.147
TP332R	Upper Devonian	0.197	0.290	−0.001	0.174	0.219	0.121
TP364R	Upper Silurian	0.475	0.087	0.009	0.204	0.177	0.049
TP374R	Upper Devonian	0.114	0.353	0.105	0.128	0.168	0.132
TP375R	Lower Devonian	0.066	0.252	0.019	0.414	0.038	0.211
TP379R	Lower Devonian	0.123	0.330	0.041	0.223	0.078	0.205
TP383R	Lower Carboniferous	0.269	0.102	0.050	0.235	0.160	0.184
TP397R	Upper Devonian	0.134	0.279	0.016	0.194	0.211	0.167
TP405R	Lower Devonian	0.017	0.492	0.017	0.129	0.103	0.242
TP415R	Middle Devonian	0.320	0.143	0.004	0.224	0.146	0.164
TP428R	Upper Devonian*	0.117	0.132	0.120	0.240	0.255	0.137
TP430R	Upper Devonian*	0.208	0.012	0.168	0.229	0.245	0.138
TP447R	Lower Devonian	0.531	−0.051	−0.015	0.226	0.157	0.153
TP453R	Upper Devonian	0.264	0.191	−0.012	0.241	0.186	0.130
TP458R	Lower Devonian	0.303	0.053	0.083	0.204	0.180	0.177
TP465R	Upper Devonian	0.219	0.152	0.069	0.168	0.218	0.175
TP505R	Middle Devonian	0.313	0.195	−0.003	0.184	0.135	0.176
TP507R	Middle Devonian	0.391	0.126	−0.001	0.196	0.150	0.137
TP519R	Middle Devonian	0.246	0.277	0.013	0.164	0.062	0.238
TP520R	Middle Devonian	0.235	0.314	0.007	0.160	0.101	0.182
TP540R	Silurian	0.199	0.004	0.218	0.188	0.137	0.253
TP544R	Silurian	0.174	0.278	0.055	0.119	0.027	0.347
TP565R	Silurian	0.451	0.125	0.005	0.173	0.143	0.103
TP569R	Upper Devonian	0.092	0.291	0.130	0.142	0.179	0.166
TP570R	Upper Devonian	0.124	0.202	0.194	0.120	0.144	0.218
TP571R	Upper Devonian*	0.089	0.230	0.066	0.170	0.167	0.276
TP572R	Upper Devonian*	0.229	0.174	0.134	0.142	0.138	0.182
TP574R	Lower Devonian	0.174	0.199	0.022	0.181	0.175	0.249

Table 2. Continued

Sample	Age	EM 1 Waxy	EM 2 Cyanobacteria	EM 3 Biodegradation	EM 4 *G. prisca*	EM 5 Open-Marine	EM 6 Microbial
TP599R	Upper Devonian*	0.130	0.281	0.127	0.146	0.168	0.149
TP606R	Upper Devonian	0.145	0.244	0.074	0.156	0.143	0.238
TP610R	Upper Devonian	0.358	−0.043	0.181	0.294	0.021	0.189
TP611R	Upper Silurian	−0.007	0.424	0.055	0.116	0.046	0.367
TP613R	Upper Silurian	0.078	0.189	0.023	0.186	0.180	0.345
TP615R	Upper Silurian	0.140	0.260	0.162	0.131	0.164	0.143
TP635R	Upper Permian	0.071	0.367	0.059	0.149	0.161	0.194
TP637R	Lower Devonian	0.382	0.196	0.067	0.168	0.067	0.120
TP642R	Upper Devonian	0.253	0.175	0.175	0.154	0.134	0.110
TP643R	Upper Devonian*	0.146	0.260	0.133	0.147	0.164	0.150
TP651R	Upper Devonian	0.137	0.242	0.163	0.150	0.137	0.171
TP653R	Lower Carboniferous	0.177	0.293	0.094	0.197	0.148	0.091
TP658R	Lower Devonian	0.139	0.457	0.027	0.130	0.103	0.145
TP667R	Upper Devonian	0.069	0.289	0.150	0.172	0.119	0.202
TP669R	Upper Devonian	0.247	0.197	0.040	0.151	0.190	0.175
TP674R	Upper Devonian	0.092	0.186	0.193	0.134	0.164	0.232
TP675R	Upper Devonian*	0.146	0.243	0.137	0.131	0.190	0.154
TP676R	Upper Devonian*	0.164	0.226	0.141	0.133	0.189	0.148
TP677R	Upper Devonian	0.320	0.252	0.036	0.188	0.012	0.191
TP680R	Upper Devonian	0.173	0.255	0.131	0.149	0.164	0.129
TP688R	Upper Devonian	0.232	0.224	−0.025	0.180	0.232	0.156
TP699R	Upper Devonian*	0.116	0.321	0.113	0.130	0.182	0.139
TP745R	Middle Devonian	0.281	0.118	0.004	0.267	0.134	0.197
TP746R	Middle Devonian	0.132	0.187	0.143	0.136	0.164	0.239
TP748R	Middle Devonian	0.421	0.151	0.009	0.163	0.121	0.135
TP754R	Middle Devonian	0.437	0.109	−0.019	0.196	0.133	0.143
TP760R	Middle Devonian	0.333	0.175	−0.010	0.214	0.147	0.142
TP771R	Lower Devonian	0.293	0.106	0.091	0.210	0.168	0.132
TP775R	Middle Devonian	0.530	0.003	−0.023	0.189	0.175	0.127
TP781R	Upper Devonian	0.490	0.064	−0.019	0.173	0.154	0.138
TP785R	Upper Devonian	0.081	0.150	0.030	0.322	0.191	0.226
TP787R	Upper Devonian	0.122	0.180	0.112	0.098	0.234	0.253
TP789R	Upper Devonian*	0.144	0.095	0.090	0.192	0.196	0.283
TP790R	Upper Devonian*	0.088	0.285	0.079	0.157	0.144	0.246
TP791R	Upper Devonian*	0.120	0.240	0.086	0.183	0.195	0.176
TP001C	Lower Carboniferous	0.280	0.002	0.119	0.257	0.319	0.024
TP002C	Lower Carboniferous	0.258	0.013	0.120	0.242	0.345	0.024
TP003C	Lower Carboniferous	0.175	0.134	0.106	0.224	0.285	0.076
TP004C	Upper Devonian	0.253	0.303	0.101	0.144	0.127	0.072
TP005C	Lower Silurian	0.201	0.355	0.068	0.179	0.105	0.092
TP006C	Upper Devonian	0.173	0.271	0.088	0.253	0.101	0.114
TP007C	Middle Devonian	0.263	0.297	0.064	0.157	0.100	0.120
TP008C	Upper Devonian	0.210	0.284	0.108	0.143	0.152	0.103
TP009C	Upper Devonian	0.215	0.291	0.104	0.141	0.145	0.105
TP010C	Upper Devonian	0.224	0.274	0.098	0.149	0.149	0.107
TP011C	Middle Devonian	0.449	0.183	0.011	0.156	0.100	0.102
TP013C	Lower Permian	0.337	0.253	0.014	0.178	0.101	0.118

Table 2. Continued

Sample	Age	EM 1 Waxy	EM 2 Cyanobacteria	EM 3 Biodegradation	EM 4 *G. prisca*	EM 5 Open-Marine	EM 6 Microbial
TP014C	Middle Devonian	0.555	0.073	−0.004	0.212	0.006	0.158
TP015C	Upper Permian	0.324	0.250	0.022	0.173	0.103	0.128
TP016C	Upper Permian	0.323	0.256	0.021	0.175	0.107	0.119
TP017C	Lower Permian	0.169	0.389	0.050	0.211	0.080	0.100
TP019C	Upper Devonian	0.233	0.250	0.136	0.135	0.148	0.098
TP020C	Lower Permian	0.194	0.257	0.062	0.161	0.162	0.165
TP021C	Lower Permian	0.184	0.246	0.065	0.164	0.185	0.155
TP022C	Upper Permian	0.218	0.244	0.093	0.145	0.170	0.131
TP023C	Upper Permian	0.181	0.221	0.118	0.161	0.173	0.146
TP024C	Upper Devonian	0.244	0.251	0.112	0.140	0.150	0.103
TP025C	Upper Permian	0.173	0.320	0.063	0.139	0.185	0.121
TP026C	Upper Devonian	0.253	0.290	0.090	0.134	0.143	0.091
TP027C	Upper Devonian	0.260	0.121	0.196	0.153	0.141	0.129
TP028C	Middle Devonian	0.200	0.294	0.100	0.142	0.152	0.112
TP029C	Middle Devonian	0.407	0.187	0.011	0.157	0.131	0.107
TP030C	Upper Devonian	0.235	0.246	0.131	0.135	0.148	0.105
TP031C	Middle Devonian	0.228	0.259	0.128	0.137	0.152	0.096
TP032C	Lower Silurian	0.230	0.162	0.172	0.122	0.169	0.146
TP033C	Upper Devonian	0.210	0.261	0.102	0.175	0.122	0.131
TP035C	Upper Devonian	0.255	0.095	0.099	0.161	0.199	0.190
TP036C	Lower Devonian	0.209	0.265	0.077	0.131	0.179	0.139
TP037C	Upper Devonian	−0.019	0.583	0.068	0.125	0.040	0.203
TP038C	Upper Devonian	−0.018	0.574	0.068	0.127	0.043	0.206
TP040C	Upper Devonian	0.139	0.291	0.120	0.127	0.166	0.158
TP041C	Upper Devonian	0.428	0.149	0.005	0.155	0.143	0.121
TP042C	Middle Devonian	0.181	0.334	0.052	0.216	0.080	0.138
TP043C	Upper Permian	0.181	0.341	0.060	0.208	0.085	0.126
TP044C	Upper Devonian	0.249	0.350	0.039	0.115	0.106	0.142
TP045C	Lower Devonian	0.161	0.456	0.015	0.207	0.070	0.090
TP046C	Upper Devonian	0.194	0.426	0.058	0.068	0.032	0.222
TP047C	Upper Permian	0.107	0.239	0.082	0.183	0.196	0.194
TP048C	Lower Permian	0.133	0.299	0.067	0.160	0.186	0.156
TP052C	Upper Devonian	0.235	0.333	0.015	0.139	0.160	0.118
TP053C	Upper Devonian	0.238	0.359	0.063	0.087	0.076	0.177
TP055C	Middle Devonian	0.222	0.395	0.015	0.154	0.119	0.097
TP056C	Middle Devonian	0.234	−0.035	0.036	0.257	0.186	0.323
TP057C	Middle Devonian	0.243	0.264	0.098	0.135	0.150	0.110
TP058C	Middle Devonian	0.228	0.355	0.035	0.141	0.099	0.141
TP059C	Upper Devonian	0.144	0.372	0.083	0.137	0.173	0.091
TP060C	Upper Devonian	0.209	0.227	0.146	0.122	0.169	0.127
TP061C	Upper Devonian	0.220	0.256	0.098	0.133	0.166	0.128
TP062C	Upper Devonian	0.285	0.281	0.051	0.142	0.134	0.107
TP063C	Middle–Upper Carboniferous	0.201	0.303	0.063	0.135	0.178	0.120
TP064C	Middle Carboniferous	0.222	0.309	0.018	0.138	0.187	0.125
TP065C	Upper Carboniferous	0.167	0.163	0.082	0.199	0.202	0.188
TP066C	Lower Silurian	0.288	0.319	0.059	0.144	0.061	0.130

Table 2. Continued

Sample	Age	EM 1 Waxy	EM 2 Cyanobacteria	EM 3 Biodegradation	EM 4 *G. prisca*	EM 5 Open-Marine	EM 6 Microbial
TP067C		0.253	0.188	0.135	0.126	0.165	0.133
TP068C	Upper Devonian	0.200	0.282	0.086	0.132	0.177	0.123
TP069C	Upper Devonian	0.197	0.278	0.088	0.137	0.181	0.119
TP070C	Upper Devonian	0.214	0.304	0.073	0.135	0.169	0.105
TP071C	Upper Devonian	0.183	0.276	0.115	0.131	0.176	0.119
TP072C	Upper Carboniferous	0.194	0.280	0.089	0.133	0.178	0.126
TP073C	Lower Silurian	0.205	0.324	0.083	0.178	0.107	0.102
TP074C	Upper Devonian	0.144	0.422	0.037	0.154	0.127	0.116
TP075C	Upper Devonian	0.120	0.350	0.125	0.134	0.163	0.109
TP076C	Upper Devonian	0.191	0.384	0.065	0.152	0.073	0.134
TP077C	Lower Devonian	0.165	0.383	0.069	0.149	0.070	0.164
TP078C	Upper Devonian	0.208	0.287	0.084	0.134	0.172	0.115
TP079C	Upper Permian	0.251	0.222	0.134	0.191	0.143	0.059
TP080C	Upper Devonian	0.211	0.279	0.087	0.138	0.171	0.115
TP081C	Upper Devonian	0.470	0.160	0.009	0.164	0.084	0.114
TP083C	Lower Silurian	0.200	0.324	0.072	0.184	0.106	0.114
TP084C	Lower Carboniferous	0.229	0.321	0.090	0.144	0.113	0.104
TP085C	Lower Devonian	0.349	0.255	0.060	0.138	0.043	0.155
TP086C	Upper Silurian	0.159	0.434	0.031	0.202	0.048	0.126
TP087C	Upper Silurian	0.199	0.274	0.126	0.131	0.150	0.119
TP089C	Lower Devonian	0.220	0.343	0.026	0.154	0.096	0.162
TP090C	Lower Devonian	0.234	0.261	0.116	0.138	0.134	0.118
TP091C	Lower Devonian	0.151	0.452	0.011	0.208	0.077	0.101
TP092C	Lower Devonian	0.117	0.409	0.035	0.256	0.051	0.132
TP094C	Lower Devonian	0.105	0.410	0.012	0.311	0.060	0.102
TP095C	Lower Devonian	0.128	0.471	0.017	0.197	0.060	0.126
TP096C	Middle Devonian	0.216	0.310	0.062	0.183	0.068	0.161
TP097C	Upper Devonian	0.192	0.424	0.013	0.180	0.089	0.103
TP098C	Upper Devonian	0.231	0.251	0.076	0.168	0.115	0.160
TP099C	Upper Devonian	0.258	0.211	0.146	0.125	0.156	0.104
TP100C	Upper Devonian	0.234	0.225	0.111	0.130	0.178	0.122
TP101C	Upper Devonian	0.240	0.187	0.090	0.168	0.165	0.150
TP102C	Upper Devonian	0.247	0.305	0.031	0.186	0.121	0.110
TP103C	Upper Devonian	0.303	0.228	0.058	0.158	0.117	0.136
TP104C	Upper Devonian	0.209	0.294	0.058	0.130	0.183	0.126
TP105C	Lower Carboniferous	0.191	0.368	0.030	0.224	0.065	0.123
TP106C	Upper Carboniferous	0.184	0.102	0.079	0.217	0.243	0.176
TP107C	Lower Permian	0.104	0.223	0.076	0.200	0.207	0.191
TP110C	Lower Triassic	0.111	0.283	0.073	0.178	0.190	0.166
TP111C	Upper Permian	0.128	0.357	0.069	0.167	0.140	0.139
TP112C	Upper Devonian	0.267	0.293	0.031	0.176	0.111	0.122
TP113C	Upper Devonian	0.294	0.266	0.018	0.159	0.135	0.128
TP114C	Lower Permian	0.142	0.321	0.063	0.147	0.168	0.160
TP115C	Upper Devonian	0.280	0.244	0.061	0.149	0.137	0.129
TP116C	Upper Devonian	0.333	0.174	0.045	0.135	0.118	0.196
TP117C	Lower Devonian	0.299	0.277	0.031	0.140	0.112	0.141
TP118C	Silurian	0.213	0.337	0.035	0.143	0.118	0.155

Table 2. Continued

Sample	Age	EM 1 Waxy	EM 2 Cyanobacteria	EM 3 Biodegradation	EM 4 *G. prisca*	EM 5 Open-Marine	EM 6 Microbial
TP119C	Upper Devonian	0.257	0.280	0.048	0.135	0.141	0.138
TP120C	Upper Devonian	0.246	0.295	0.049	0.138	0.140	0.133
TP121C	Lower Permian	0.168	0.242	0.070	0.164	0.171	0.185
TP122C	Upper Permian	0.085	0.253	0.075	0.177	0.219	0.191
TP123C	Lower Permian	0.198	0.172	0.070	0.176	0.174	0.211
TP124C	Lower Permian	0.193	0.226	0.069	0.170	0.179	0.163
TP125C	Lower Triassic	0.109	0.432	0.050	0.142	0.161	0.106
TP126C	Upper Devonian	0.290	0.293	0.029	0.124	0.110	0.155
TP127C	Upper Devonian	0.286	0.308	0.028	0.113	0.107	0.157
TP128C	Lower Devonian	0.245	0.317	0.060	0.199	0.054	0.126
TP131C	Lower Devonian	0.186	0.412	0.012	0.232	0.059	0.100
TP132C	Lower Devonian	0.194	0.401	0.018	0.234	0.030	0.124
TP133C	Lower Devonian	0.355	0.197	0.033	0.206	0.050	0.158
TP134C	Upper Devonian	0.268	0.300	0.030	0.175	0.108	0.119
TP135C	Upper Devonian	0.288	0.149	0.095	0.129	0.158	0.180
TP136C	Upper Carboniferous	0.231	0.163	0.047	0.179	0.252	0.128
TP137C	Lower Triassic	0.117	0.437	0.052	0.134	0.155	0.105
TP138C	Lower Devonian	0.291	0.260	0.064	0.159	0.062	0.165
TP140C	Upper Devonian	0.305	0.206	0.039	0.117	0.103	0.230
TP141C	Upper Devonian	0.277	0.262	0.025	0.115	0.112	0.210
TP143C		0.205	0.385	0.055	0.070	0.033	0.251
TP144C	Upper Devonian	0.247	0.324	0.057	0.085	0.018	0.268
TP145C	Upper Devonian	0.320	0.247	0.036	0.124	0.099	0.173
TP146C	Devonian	0.261	0.214	0.101	0.138	0.158	0.129
TP147C	Upper Carboniferous	0.141	0.317	0.110	0.176	0.155	0.101
TP148C	Lower Permian	0.148	0.204	0.128	0.184	0.157	0.180
TP149C	Upper Devonian	0.196	0.381	0.029	0.209	0.072	0.113
TP150C	Lower Devonian	0.164	0.428	0.013	0.195	0.086	0.114
TP151C	Lower Devonian	0.174	0.379	0.055	0.200	0.060	0.132
TP152C	Lower Permian	0.131	0.314	0.090	0.165	0.154	0.146
TP153C	Silurian	0.125	0.441	0.020	0.238	0.050	0.126
TP154C	Lower Triassic	0.161	0.089	0.108	0.198	0.174	0.271
TP155C	Lower Devonian	0.145	0.463	0.013	0.195	0.083	0.100
TP156C	Upper Carboniferous	0.154	0.112	0.081	0.211	0.203	0.239
TP157C	Upper Devonian	0.244	0.229	0.102	0.133	0.161	0.130
TP158C	Lower Permian	0.161	0.281	0.066	0.156	0.169	0.166

*Domanik facies.

Fowler and Douglas, 1987; Shiea et al., 1990; Summons and Walter, 1990). These peaks do not appear in the same relative proportion in crude oils with high values of EM 2 (Figure 5b). However, the similarity in the shape of the alkane profiles from rocks and oils high in EM 2 suggests a common biogenic source (Figure 5). Hence, we conclude that cyanobacteria are a major source for EM 2.

Cyanobacteria have been considered a possible source of monomethyl alkanes in ancient sediments and crude oils since their identification in the extractable lipids of cyanobacterial cultures (Han et al., 1968; Gelpi et al., 1970; Fowler and Douglas, 1987; Shiea et al., 1990; Summons and Walter, 1990). The emergence of EM 2 in our analysis suggests significant cyanobacterial biological sources in our source rocks and crude oils,

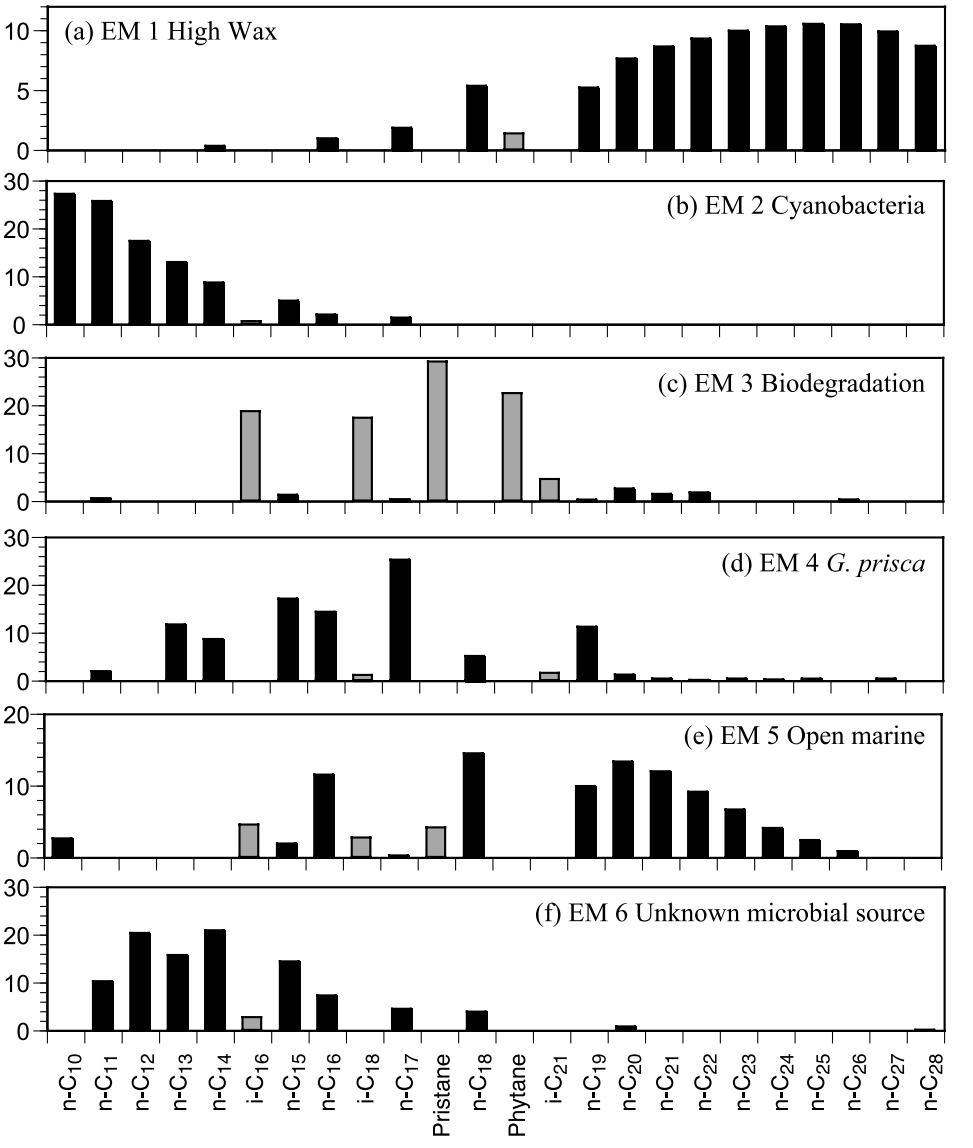

Figure 1. Histograms showing the chemical composition of end members (EM) derived from crude oils and rock extracts from the Timan-Pechora basin: (a) EM 1 = high wax; (b) EM 2 = cyanobacterial lipids; (c) EM 3 = moderate biodegradation; (d) EM 4 = *G. prisca* (e) EM 5 = open-marine algal/bacterial organic material; (f) EM 6 = microbial source. Black bars represent relative abundances of the n-alkanes, gray bars represent relative abundances of the acyclic isoprenoids.

about 20 and 28% on average, respectively. Cyanobacteria would appear to be the major biological sources to TP40R B (49%) and TP037C (58%).

EM 3 (Biodegradation/Weathering)

End member 3 is a spectrum representing the intermediate stage of biodegradation (Table 1; Figure 1c). Because samples subjected to more severe levels of biodegradation are largely devoid of n-alkanes and acyclic isoprenoids, they were excluded from the data set prior to our statistical analysis. EM 3 (Figure 1c) contains abundant acyclic isoprenoids and low amounts of the C_{17} to C_{26} n-alkanes. EM 3 has a pristane-to-phytane ratio of 1.3. The elevated abundance of acyclic isoprenoids relative to n-alkanes is consistent with preferential removal of the straight-chain compounds during early stages of biodegradation (Shanmugam, 1985; Peters and Moldowan, 1993). Mixing proportions for EM 3 are low in both rock extracts and crude oils, from 0 to 22% (mean, 6%) for source rocks and 0 to 20% (mean, 7%) for oils. Samples with relatively high amounts of EM 3 (>10%) display an elevated baseline on the GC-FID traces because of the enrichment of the unresolved complex mixture. Rock extracts collected from outcrop tend to display relatively high levels of weathering (i.e., elevated levels of EM 3). Contributions of EM 3 to the crude oils appear to be independent of reservoir age or the producing interval (depth in meters; Table 2).

EM 4 (*G. prisca*)

A predominance of C_{13} to C_{19} n-alkanes with a strong odd-carbon preference and a low abundance of C_{20}^{+}

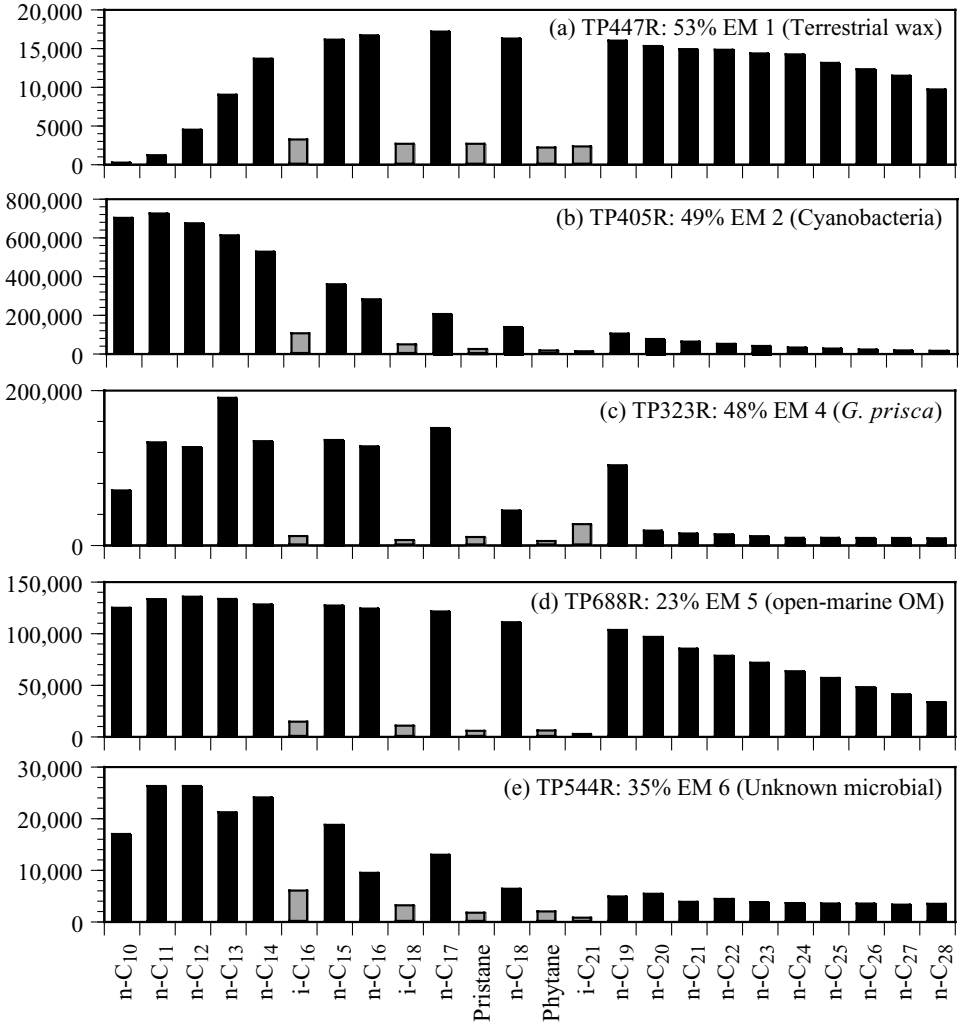

Figure 2. Histograms showing the chemical compositions (integrated peak area vs. compound) for Timan-Pechora rock extracts that contain maximum proportions of each end members as defined in Figure 1: (a) high-wax rock extract (TP447B; Middle Devonian); (b) cyanobacterial lipid-rich rock extract (TP405R; Lower Permian); (c) rock extract rich in the *G. prisca* chemical signature (TP323R; Lower Devonian); (d) rock extract containing predominantly open-marine algal and bacterial lipids (TP688R; Upper Devonian); (e) rock extract with a significant unknown microbial chemical signature (TP544R; Silurian). Black bars represent relative abundances of the n-alkanes, gray bars represent relative abundances of the acyclic isoprenoids.

n-alkanes characterize EM 4. The acyclic isoprenoids i-C_{18} and i-C_{21} are present in trace amounts, and pristane and phytane are absent from this end member (Figures 1d, 2c, 3c, 6). These features are typical of crude oils generated from Ordovician source rocks throughout the world that contain significant amounts of the microbial organism *G. prisca* (Reed et al., 1986; Hatch et al., 1987; Derenne et al., 1990; Stasiuk et al., 1993). *G. prisca* is a colonial microorganism whose inferred lipid signature is commonly observed in shale extracts and crude oils generated from Ordovician source rocks worldwide (Fowler and Douglas, 1984; Requejo et al., 1995). Source rocks containing abundant *G. prisca* generate high amounts of n-alkanes during flash pyrolysis with the diagnostic fingerprint similar to EM 4 (Douglas et al., 1991). Derenne et al. (1992) clearly demonstrated that this extinct marine microalga is very likely related to the freshwater green microalga *Botryococcus braunni* race A, an algae known to generate high amounts of a well-characterized algaenan (Metzger et al., 1991). This indicates that marine microalgae related to the present species existed in the geologic past and were able to biosynthesize algeanans.

Although the microbial organism *G. prisca* is generally associated with marine-source facies of Ordovician age, the characteristic chemical fingerprint of *G. prisca* also has been observed in Silurian and Lower Devonian rocks in the Pechora basin (Abrams et al., 1999). Indeed, rock extracts containing the highest mixing proportions of EM 4 are generally confined to Devonian shale extracts (Table 2). The extract from TP323R contains more than 48% EM 4 and is the closest to the pure end member in the data set (Figures 2c, 6a).

The produced oils are less variable than the rock extracts with maximum mixing proportions of 34.5% EM 4. The GC-FID traces of the crude oils with approximately 20% EM 4 display strong characteristics of *G. prisca*: a predominance of middle-range n-alkanes

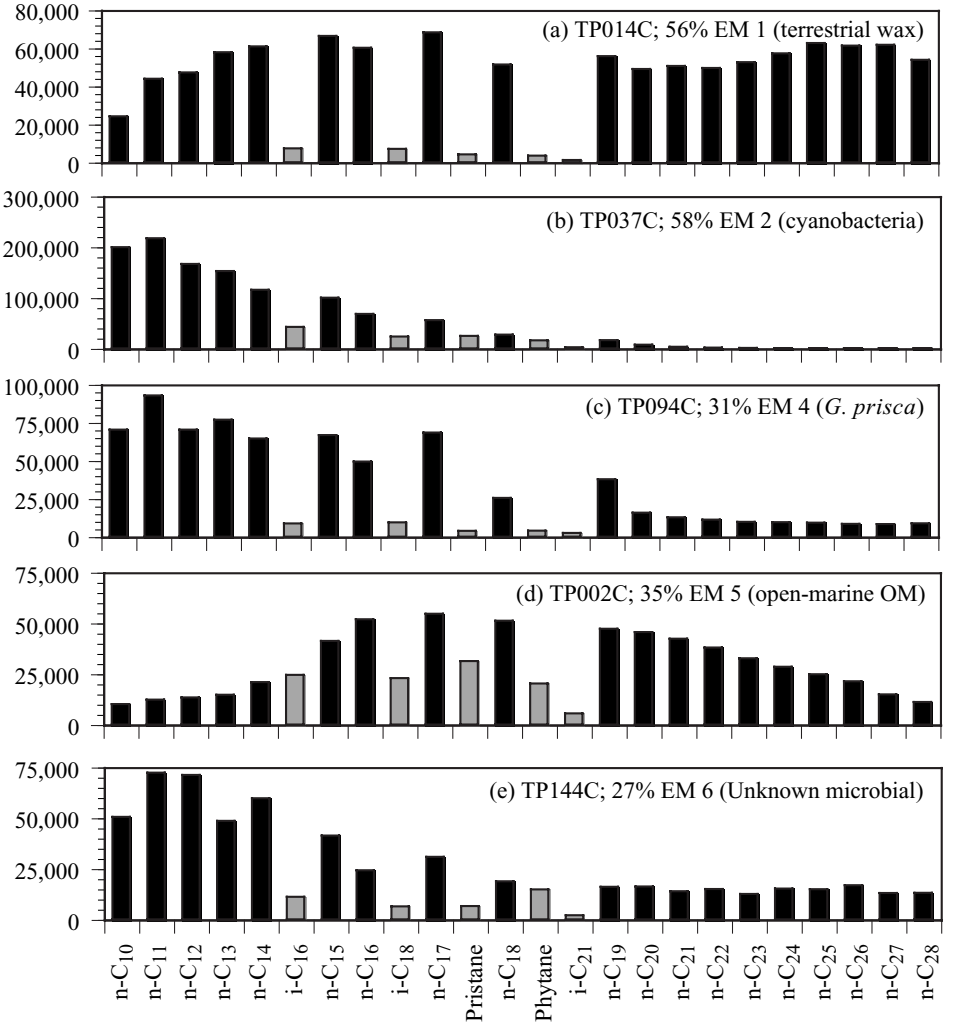

Figure 3. Histograms showing the chemical compositions (integrated peak area vs. compound) for Timan-Pechora crude oils that contain the highest proportion of each end member described in Figure 1: (a) high-wax crude oil (TP014C); (b) cyanobacterial lipid-rich crude oil (TP037C); (c) crude oil rich in the *G. prisca* chemical signature (TP094C); (d) crude oil containing predominantly open-marine algal and bacterial lipids (TP002C); (e) crude oil with a significant unknown microbial chemical signature (TP144C). Black bars represent relative abundances of the n-alkanes, gray bars represent relative abundances of the acyclic isoprenoids.

with an odd-carbon preference in the range of n-C_{13} to n-C_{19} (Figure 6). These oils are produced from Silurian to Upper Permian reservoirs, with most samples clustering in the Lower Devonian. This is consistent with previous studies where G. *prisca* type oils were found in Carboniferous–Lower Devonian reservoirs in the northern portion of the Timan-Pechora basin (Requejo et al., 1995; Abrams et al., 1999).

EM 5 (Open-Marine Algal/Bacterial Material)

EM 5 is assigned to algal/bacterial organic detritus deposited in a relatively oxidizing, open-marine setting (Figures 1e, 2d, 3d, 7). EM 5 displays abundant n-alkanes from C_{18} to C_{28} and a unimodal envelope with a maximum at n-C_{20}; the long-chain homologs show a near-linear decrease with increasing carbon number (Figures 1e, 7). The acyclic isoprenoids i-C_{16}, norpristane (i-C_{18}), and pristane are present in moderately low abundance, and the higher homologs are absent. The dominance of middle-range n-alkanes is consistent with input from heterotrophic bacteria that metabolize organic material from primary producers (Han et al., 1968; Jones, 1969; Jones and Young, 1970; Han et al., 1980; Collister et al., 1994). Pyrolysates of isolated kerogenlike material isolated from Black Sea sediments display n-alkane profiles very similar to that of this end member and samples containing elevated mixing proportions of EM 5 (Garcette-Lepecq et al., 2000). These authors concluded that selective preservation of terrigenous material, as well as resistant aliphatic biomarcromolecules (probably derived from the cell walls of algae), was the main process for the formation of this material, which accounted for as much as 50% of the organic matter in these sediments.

Proportions of EM 5 in the rocks range from 0.12 to 25.5% (average = 14.8%). Three-quarters of the rock extracts show EM 5 ranging between 10 and 20%. This

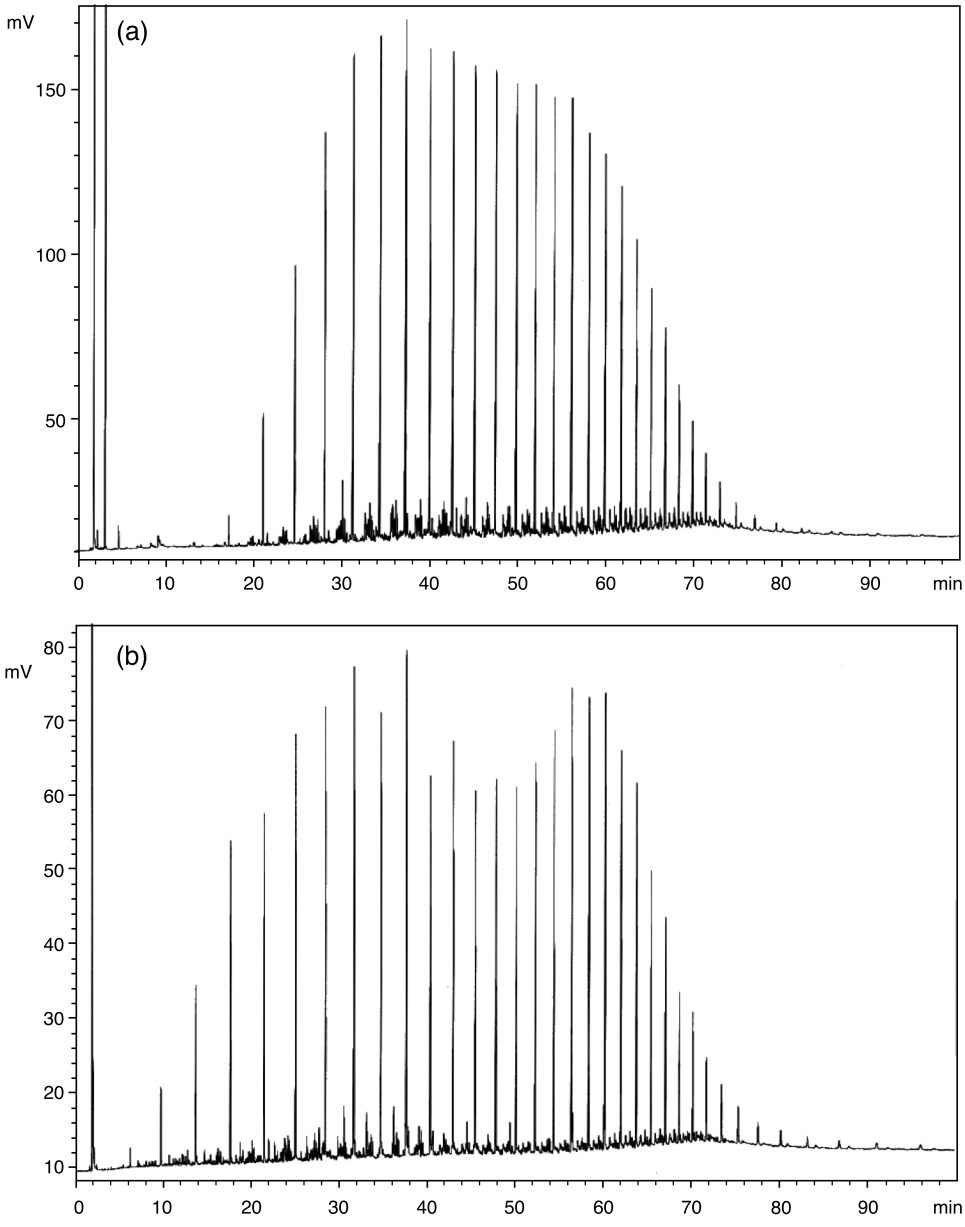

Figure 4. GC-FID traces for a rock extract (a) TP447B and crude oil (b) TP014C that contains a high abundance of the terrestrial wax end member (EM 1).

suggests that an open-marine setting was relatively constant throughout the Devonian. Mixing proportions of EM 5 in the crude oils are about the same, ranging from 0.6 to nearly 35%, with an average value of 13%. Sixty-five percent of the crude samples contain between 10 and 20% EM 5. Proportions of EM 5 above 17% are found predominantly in Permian to Triassic reservoirs (Table 2).

EM 6 (Unknown Microbial Source)

EM 6 contains mainly middle-range n-alkanes in the carbon number range C_{11} to C_{18} and low amounts of C_{19}^{+} n-alkanes. A pronounced even-carbon preference is observed at n-C_{12} and n-C_{14}. The acyclic isoprenoids are absent from the end member except for the C_{16} homolog (Figures 1f, 2e, 3e, 8). Lipids from algae and bacteria are commonly dominated by straight-chain components in this carbon number range (Han et al., 1968; Han and Calvin, 1969; Gelpi et al., 1970), suggesting a microbial origin for this end member. The distribution pattern of the n-alkanes in EM 6 shows a striking similarity to pyrolysis gas chromatography–mass spectrometry traces obtained from solvent-extracted residues of dinoflagellates (Gelin et al., 1999). We suggest that thermal breakdown of biopolymers derived from dinoflagellates or similar microbial primary producers are the biological source for this end member.

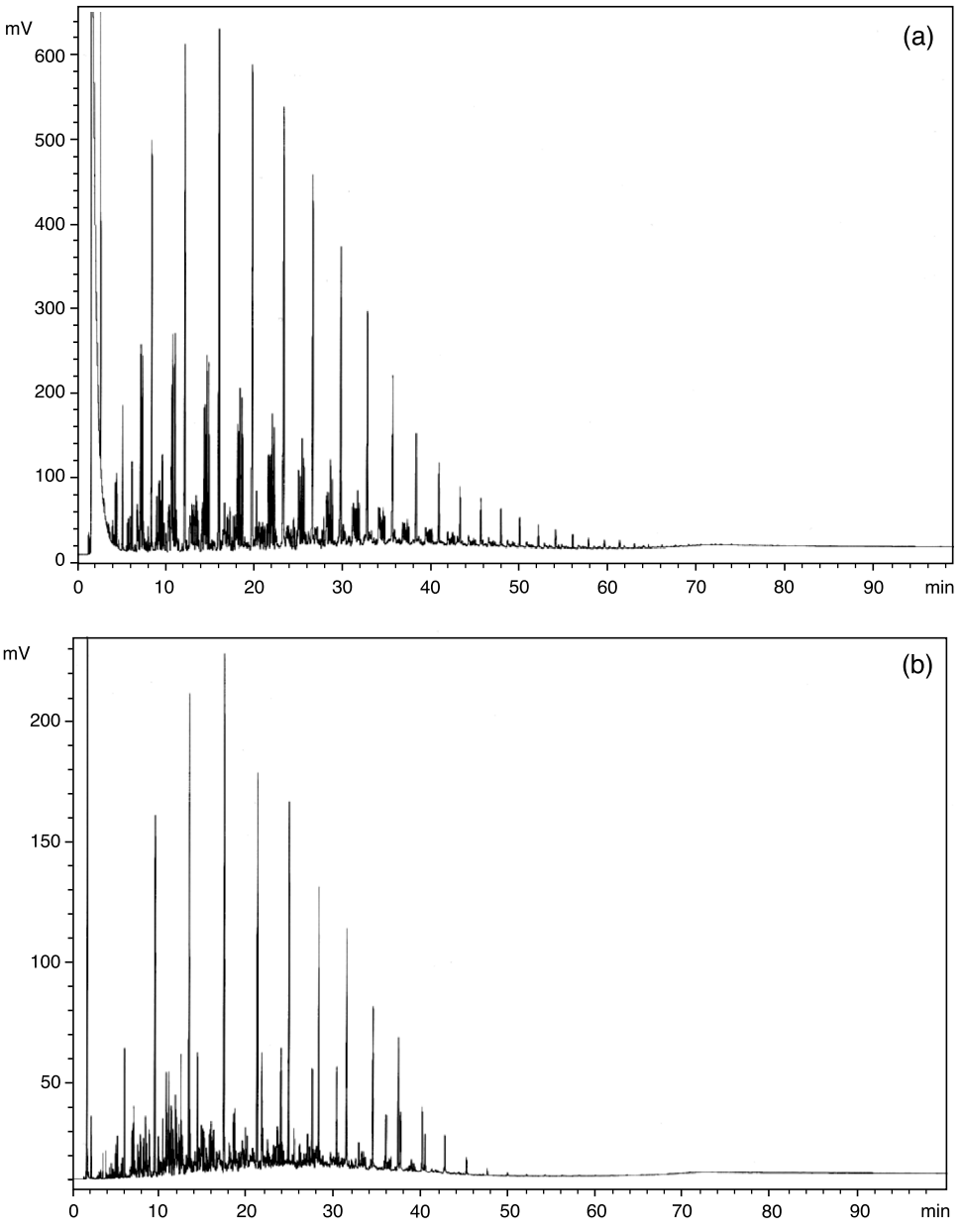

Figure 5. GC-FID traces for a rock extract (a) TP405B and crude oil (b) TP037C that contains a high abundance of the cyanobacteria end member (EM 2). Several significant series of diagnostic peaks eluting between the more prominent n-alkanes are monomethyl alkanes, characteristic of cyanobacteria.

Proportions of EM 6 in rock extracts range from 5 to more than 36%, with an average value of 18%. Samples with more than 30% of this end member are restricted to the Silurian interval (TP544R, TP611R, and TP613R; Table 2). Proportions of EM 6 in the crude oils are generally lower, with a range of 2.4–32% and an average value of 14% (Table 2).

DISCUSSION

The alkane/isoprenoid spectra in our database of oils and source rock extracts are duplicated by linear combinations of six subspectra (end members). Only one end member represents postgeneration alteration (EM 3, biodegradation). The others reflect distinct biological sources (biological provenance). Their spectra, therefore, are viewed as primary spectra. Oil mixing from different source rocks could explain the observed blend of end members in our oil set. However, the same end members appear in rock extracts where oil mixing is unlikely, suggesting that the kerogen of any given source rock is comprised of a mixture of biopolymers from multiple biological sources.

We could not find in any end member in our analysis a signal that can be ascribed to a general process of destructive distillation of kerogen, although we did derive one that represents the destructive effect of

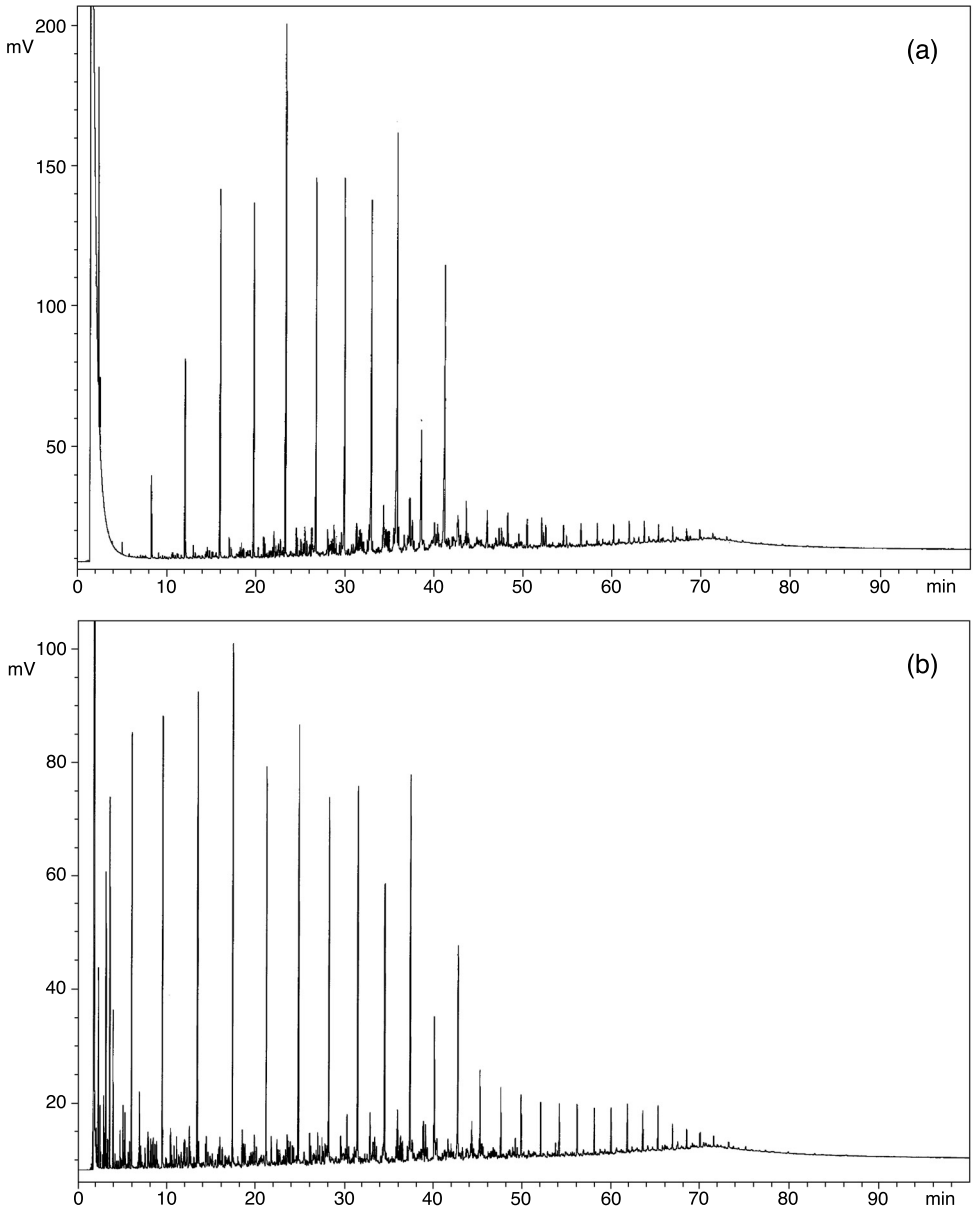

Figure 6. GC-FID traces for a rock extract (a) TP323B and crude oil (b) TP094C that contains a high abundance of the *G. prisca* end member (EM 4).

biodegradation in the reservoir. This is surprising in that the source rocks and oils were subjected to differences in time and temperature regimes. Indeed, as discussed below, it appears that the biological signal was somehow preserved in a state that resisted bacterial effects early in the sedimentation process and maturation effects to the oil window.

The waxy end member and the cyanobacteria end member are volumetrically the most important contributors to the crudes, their sum comprising more than 40% of the alkanes and isoprenoids in most samples. The presence of the waxy end member (presumably derived from higher plants) is not surprising in the light of previous studies of oil families from the Timan-Pechora basin (Requejo et al., 1995; Abrams et al., 1999). However, the existence of cyanobacteria as an important source in most samples is surprising. Cyanobacteria have long been recognized to be a potential petroleum precursor, but the extent of their contributions to oils is greater than we expected. A rough inverse relationship exists between the proportion of the waxy end member and the cyanobacteria end member, reflecting the relative dominance of a nearshore vs. an open-marine depositional setting.

The occurrence of the products of *G. prisca* in both source rocks and oils is less surprising. Although most prominent in Ordovician rocks, Tyson (1995) reports petrographic identifications of *G. prisca* in rocks as young as Silurian. Abrams et al. (1999) reported the geochemical signature of this bacterium

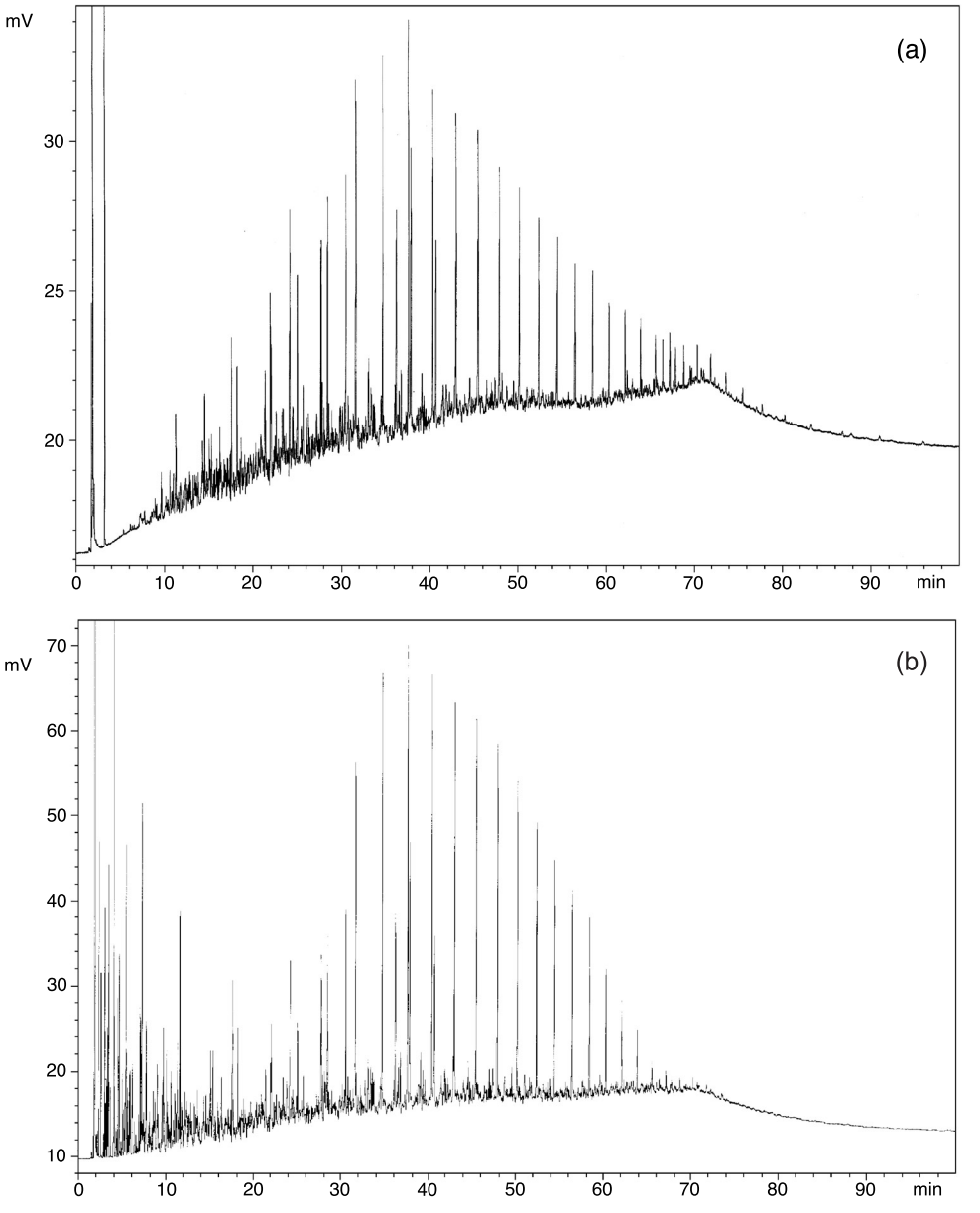

Figure 7. GC-FID traces for a rock extract (a) TP430B and crude oil (b) TP002C that contains a high abundance of the open-marine algal/bacterial organic matter end member (EM 5).

from Devonian rock extracts. We also find this fingerprint in subsidiary but significant proportions (~20%) in samples from the Lower Carboniferous. We speculate that G. *prisca* may occur over a wider range of time than this; some have even speculated that it may occur in special niches today (Tyson, 1995).

Implications and Conjectures

Our current understanding of the petroleum system is a consideration in evaluating new plays and play concepts. The alkanes and isoprenoids in the suite of crude oils discussed here can be considered to be products of the direct conversion of primary organic materials to oil. This goes against conventional wisdom that requires extensive processing of kerogen before oil is expelled, and that the expulsion process be gradual because of the complexity of the kerogen. Thus, current thinking about the petroleum system might be too restrictive. Our results raise the possibility that source rocks containing low TOC or source rocks that may have been previously considered undermature can generate significant oil if the source carries enough of a special kerogen type, a type that is derived from biological membranes that are so resistant that they are essentially unchanged until the time of liquefaction. This suggests that it might be prudent to re-evaluate undrilled basins that were rejected because TOC was thought to be too low or the source rocks did not spend sufficient time in the oil window.

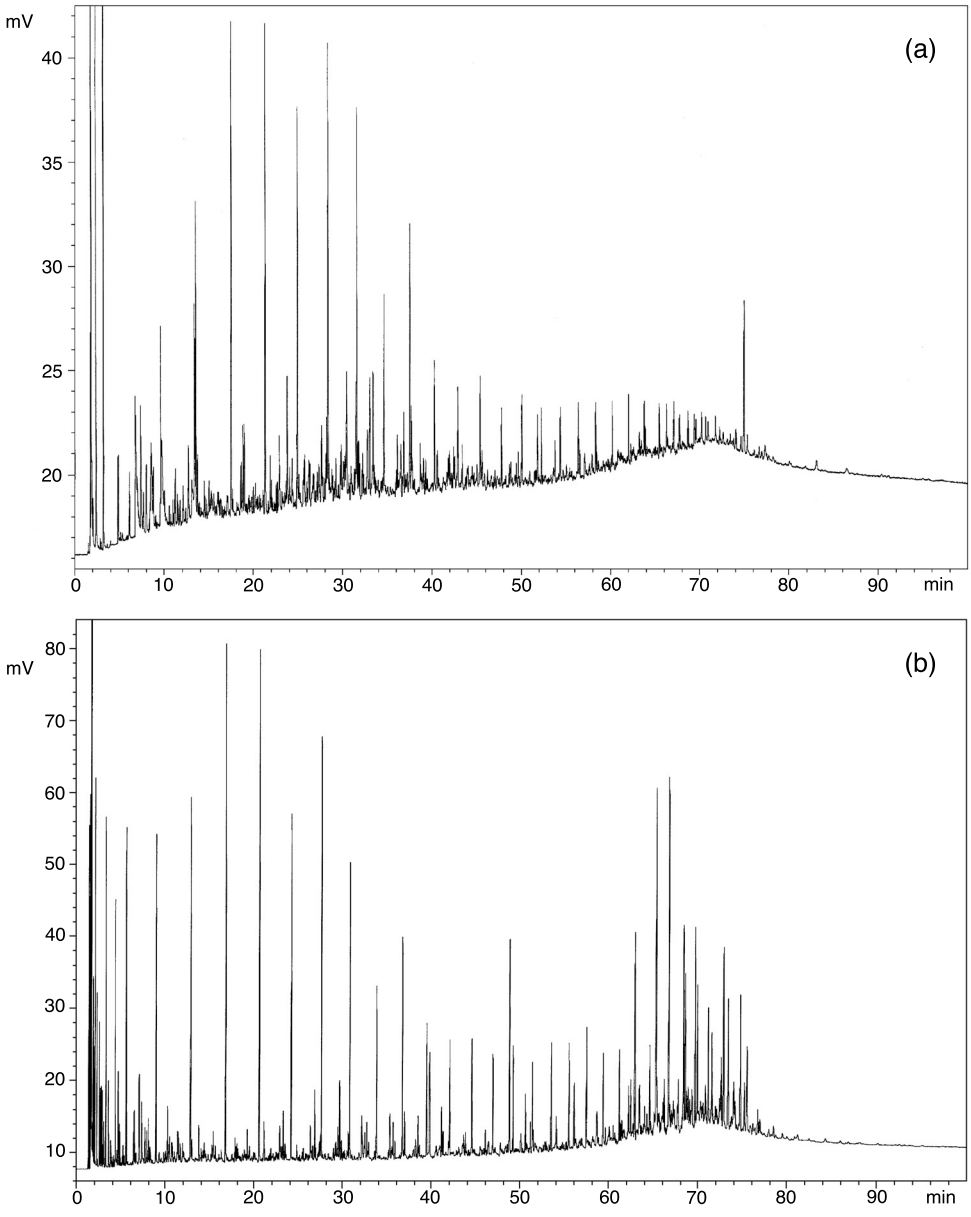

Figure 8. GC-FID traces for a rock extract (a) TP544B and crude oil (b) TP144C that contains a high abundance of a spectrum derived from an unidentified microbial source (EM 6).

These conclusions are supported by a series of observations and experiments, mostly in French laboratories, that show that resistant organic membranes in the form of biopolymers can play this role. They are stable over a large range of conditions, surviving both early secondary bacterial attack and a late-stage progressive breakdown under increasing thermal stress. Examination of the reports of microscopic observations of kerogen suggests that such biological membranes commonly constitute only a small proportion of the kerogen, although they have been shown to comprise as much as 50% of the organic matter in recent sediments from the Black Sea (Garcette-Lepecq et al., 2000). If biopolymers are generally a small portion of kerogens, then a small subfraction of the kerogen is responsible for a significant oil fraction, and by implication, the residual kerogen is basically raw material for natural gas.

Biological membranes, by virtue of their simple chemical composition and structure, liquefy at a threshold temperature and do not require a time and temperature scenario for maturation. This should ensure that a large volume of oil could be generated over a short time. A burst of oil generation can serve to produce transient overpressures resulting in liberation of oil by microfracturing and perhaps long-range migration because of creation of fractures. A rapid accumulation of large volumes of oil in a short time will also provide the collective buoyancy necessary to drive large-scale migration.

APPENDIX 1: SAMPLE INFORMATION FOR TIMAN-PECHORA POTENTIAL SOURCE ROCKS

Sample Identification	Field Name and Well Number	Depth (m)	Longitude (North)	Latitude (East)	Age
TP018R	Kyrtayel-14	3144.4–3149.9	57.04759	64.99935	Middle Devonian
TP042R	Vuktyl-58	4527–4530	57.28837	63.71286	Lower Carboniferous
TP084R	Vangurey-81	4647–4649	55.81670	68.41078	Middle(?) Devonian
TP117R	Sunayel-7	2156–2164	55.92627	64.52732	Upper Devonian
TP123R	Yugyd-59	2933–2936.8	57.33121	64.66096	Middle Devonian
TP137R	Borovaya-2	1987.2–1995	55.32403	63.62929	Upper Devonian
TP138R	Borovaya-2	2005.7–2013.7	55.32403	63.62929	Upper Devonian
TP141R	Borovaya-2	2029.3–2035.5	55.32403	63.62929	Upper Devonian
TP154R	Kharyaga-100	3364–3372	56.67928	67.20760	Upper Devonian*
TP156R	Kharyaga-100	3378.4–3384.6	56.67928	67.20760	Upper Devonian*
TP169R	Mutnyy Materik-3	2400.7–2402.7	55.34557	65.80055	Upper Devonian
TP198R	Usinsk-7	3370–3373.3	57.27971	66.23758	Lower Devonian
TP209R	Ust-Rasyu-1	1946.4–1953.5	55.50688	63.74526	Upper Devonian
TP212R	Ust-Rasyu-1	1972.5–1978.9	55.50688	63.74526	Upper Devonian
TP242R	Kharyaga-1068	3756–3764	56.71865	67.16683	Middle Devonian
TP243R	Kharyaga-1068	3783–3793	56.71865	67.16683	Middle Devonian
TP247R	Kyrtayel-18	2875–2883	56.93514	65.01720	Middle Devonian
TP298R	October (Olenya)-15	3925–3934	58.35539	68.22733	Upper Silurian
TP299R	October (Olenya)-15	3934–3941	58.35539	68.22733	Upper Silurian
TP323R	October (Olenya)-16	4036–4043	58.59140	68.32398	Lower Devonian
TP332R	Bolshezemelsk-1	4352–4363	56.90378	67.53365	Upper Devonian
TP364R	Syurkharatinsk-2	3945.6–3954.5	57.71353	67.99737	Upper Silurian
TP374R	Yareyyaga-91	3016–3018	59.57224	67.84274	Upper Devonian
TP375R	Yareyyaga-91	3150–3158	59.57224	67.84274	Lower Devonian
TP379R	East Yareyu-300	4641–4648	55.92651	67.96937	Lower Devonian
TP383R	Upper Laya-500	3192–3197	55.34803	67.37820	Lower Carboniferous
TP397R	Upper Laya-500	4050–4059	55.34803	67.37820	Upper Devonian
TP405R	Upper Laya-500	4720–4726	55.34803	67.37820	Lower Devonian
TP415R	Kyrtayel-18	2875.1–2883	56.93514	65.01720	Middle Devonian
TP428R	Chut River-7/4	outcrop	53.39925	63.53570	Upper Devonian*
TP430R	Chut River-7/6	outcrop	53.39925	63.53570	Upper Devonian*
TP447R	Inzyrey-206	4499–4506	56.52981	67.53101	Lower Devonian
TP453R	Inzyrey-206	4252–4359	56.52981	67.53101	Upper Devonian
TP458R	Malinovsk-1	4420–4434	58.28516	68.65894	Lower Devonian
TP465R	Malinovsk-1	3915–3925	58.28516	68.65894	Upper Devonian
TP505R	Khanoney-1	4692–4700	56.12033	67.60902	Middle Devonian
TP507R	Khanoney-1	4501–4505	56.12033	67.60902	Middle Devonian
TP519R	East Yareyu-301	4535–4539	55.98267	67.93520	Middle Devonian
TP520R	East Yareyu-301	4496–4505	55.98267	67.93520	Middle Devonian
TP540R	Cherpayu-3	2617.3	60.47370	67.39341	Silurian
TP544R	Cherpayu-3	3070	60.47370	67.39341	Silurian
TP565R	Kolva-1	3679.8	59.45717	67.40011	Silurian
TP569R	Kolva-4	3582.8–3591.9	59.42412	67.44779	Upper Devonian
TP570R	Kolva-4	3586.7	59.42412	67.44779	Upper Devonian
TP571R	East Pomolesshor-40	3855–3859	59.87853	67.41352	Upper Devonian*
TP572R	East Pomolesshor-40	3880–3890	59.87853	67.41352	Upper Devonian*
TP574R	East Pomolesshor-40	4060–4065	59.87853	67.41352	Lower Devonian
TP599R	Domanik River 20	outcrop	53.44536	63.50869	Upper Devonian*
TP606R	East Kolva-51	4011–4022	57.15630	67.48637	Upper Devonian
TP610R	East Vaneyvis-1	3998–4006	54.20193	67.85983	Upper Devonian
TP611R	East Vaneyvis-1	4808–4816	54.20193	67.85983	Upper Silurian
TP613R	East Vaneyvis-1	5110–5118	54.20193	67.85983	Upper Silurian
TP615R	West Lekkeyaga-65	3575–3582.3	60.25311	68.26685	Upper Silurian
TP635R	Labogey-15	4496–4501.5	62.06165	68.27742	Upper Permian
TP637R	Mezhdurechensk-1	4350–4356	59.73369	68.19946	Lower Devonian
TP642R	Osovey-46	3281–3288	60.02748	67.60101	Upper Devonian

APPENDIX 1: Continued

Sample Identification	Field Name and Well Number	Depth (m)	Longitude (North)	Latitude (East)	Age
TP643R	Osovey-46	3613–3615	60.02748	67.60101	Upper Devonian*
TP651R	Osovey-46	3281–3288	60.02748	67.60101	Upper Devonian
TP653R	Perevoznaya-6	2059.1–2064.8	59.03781	68.96686	Lower Carboniferous
TP658R	Perevoznaya-6	3862.8–3868	59.03781	68.96686	Lower Devonian
TP667R	Khosolta-95	3679–3691	60.08195	67.40853	Upper Devonian
TP669R	Khosolta-96	3750–3757	60.15326	67.35462	Upper Devonian
TP674R	South Khosedayu-1	3638–3644	58.62141	67.82787	Upper Devonian
TP675R	South Khosedayu-1	3718–3724	58.62141	67.82787	Upper Devonian*
TP676R	South Khosedayu-1	3724–3733	58.62141	67.82787	Upper Devonian*
TP677R	South Khosedayu-1	3836–3847	58.62141	67.82787	Upper Devonian
TP680R	Yaneytyvis-1	3486–3490	58.55851	67.41050	Upper Devonian
TP688R	Moroshkinsk-31	4494.1–4501.1	55.80324	67.29379	Upper Devonian
TP699R	West Osovey-70	3776–3784	59.62247	67.60995	Upper Devonian*
TP744R	Kharyaga-2	3804	56.73823	67.16181	Middle Devonian
TP745R	Kharyaga-2	3807	56.73823	67.16181	Middle Devonian
TP748R	Kharyaga-3	3606	56.63872	67.18697	Middle Devonian
TP754R	Kharyaga-3	3653.7	56.63872	67.18697	Middle Devonian
TP760R	Kharyaga-3	3873.3	56.63872	67.18697	Middle Devonian
TP771R	Myadsey-1/50	3716–3723	59.34215	68.74561	Lower Devonian
TP775R	Kharyaga-20	4149.8–4154.2	56.59892	67.13684	Middle Devonian
TP781R	Pashnya-164	2670–2674	56.43491	63.22250	Upper Devonian
TP785R	Bolshaya Lyaga-1	3854–3862	56.87427	62.99682	Upper Devonian
TP787R	South Kykayel-887	1937.5–1939.1	54.96786	63.71785	Upper Devonian
TP789R	Bolshaya Lyaga-1	3750–3757	56.87427	62.99682	Upper Devonian*
TP790R	Bolshaya Lyaga-1	3750–3757	56.87427	62.99682	Upper Devonian*
TP791R	Bolshaya Lyaga-1	3815–3823	56.87427	62.99682	Upper Devonian*

*Domanik facies.

APPENDIX 2: SAMPLE INFORMATION FOR TIMAN-PECHORA BASIN CRUDE OILS

Sample Identification	Well Name and Number	Depth (m)	Longitude (North)	Latitude (East)	Reservoir Age
TP001C	Dinyel-2	631.8–637	56.09070	62.69379	Lower Carboniferous
TP002C	Dinyel-3	655–664.5	56.08788	62.70095	Lower Carboniferous
TP003C	Dinyel-5	681–683	56.07285	62.69706	Lower Carboniferous
TP004C	Ust-Rasyu-1	1970–1976	55.50718	63.74499	Upper Devonian
TP005C	Upper Vozey-3491	3444–3514	57.10046	66.72097	Lower Silurian
TP006C	Middle Vozey-2817	2837–2883	57.01342	66.57114	Upper Devonian
TP007C	Vozey-1	3400	56.98577	66.62045	Middle Devonian
TP008C	Borovaya-2	2005	55.32341	63.62971	Upper Devonian
TP009C	Beregovaya-4	2705.5–2719	56.39116	63.33172	Upper Devonian
TP010C	Beregovaya-4	2724–2733.8	56.39116	63.33172	Upper Devonian
TP011C	Kyrtayel-8	2595	56.99237	65.00098	Middle Devonian
TP012C	Lyayel-Yarega	130	53.67753	63.35391	Middle Devonian
TP013C	Kharyaga-47	1780–1830	56.70860	67.17080	Lower Permian
TP014C	Kharyaga-1029	3640–3690	56.68356	67.18945	Middle Devonian
TP015C	Kharyaga	2670	56.79330	67.16171	Upper Permian
TP016C	Kharyaga	1670	56.79330	67.16171	Upper Permian
TP017C	Vozey	1800	56.96915	66.66775	Lower Permian
TP018C	Usinsk	1310	57.34789	66.15768	Upper Permian
TP019C	North Savinobor-157	2477	56.12833	63.72728	Upper Devonian
TP020C	South Khylchuyu-32	2160–2175	55.31757	68.16211	Lower Permian
TP021C	Khylchuyu-42	2160–2200	55.26521	68.31604	Lower Permian
TP022C	Michayu-582	580	55.83113	63.96322	Upper Permian

APPENDIX 2: Continued

Sample Identification	Well Name and Number	Depth (m)	Longitude (North)	Latitude (East)	Reservoir Age
TP023C	Pashnya-48	639–648	56.36404	63.30006	Upper Permian
TP024C	Ust-Rasyu-1	1968–1983	55.50718	63.74499	Upper Devonian
TP025C	Pashnya-603	700–740	56.42031	63.26062	Upper Permian
TP026C	Rasyu-2	1903	55.27374	63.70070	Upper Devonian
TP027C	East Savinobor-11	1456–1470	56.24787	63.56517	Upper Devonian
TP028C	Beregovaya-3	2792–2815	56.40739	63.32161	Middle Devonian
TP029C	Kyrtayel-203	2595	56.98125	65.02601	Middle Devonian
TP030C	North Savinobor	2477	56.11311	63.76321	Upper Devonian
TP031C	Michayu-9	2270–2296	55.80549	63.95297	Middle Devonian
TP032C	Usinokushshor-22	1769–1797	59.03777	66.47957	Lower Silurian
TP033C	Yurvozh-1	3980–3994	56.81136	63.10129	Upper Devonian
TP034C	Nizevolya-1	2059–2065	52.75627	65.53193	Upper Devonian
TP035C	Makaryel-1	2282–2304	53.23980	65.50996	Upper Devonian
TP036C	Kolva-11	3649–3692	59.42984	67.48366	Lower Devonian
TP037C	Sandivey-30	2920	57.65839	67.30522	Upper Devonian
TP038C	Sandivey-30	2930	57.65839	67.30522	Upper Devonian
TP039C	Padimey-21	1552	53.02744	68.51733	Lower Permian
TP040C	North Aressk-2	1819–1839	54.96137	64.36174	Upper Devonian
TP041C	Yugyd-52	3009–3036	57.33609	64.67394	Upper Devonian
TP042C	Usinsk	3043–3405	57.34789	66.15768	Middle Devonian
TP043C	Usinsk-821,934	1310	57.34002	66.20354	Upper Permian
TP044C	Yanemdey-2	3263–3285	57.46601	67.79376	Upper Devonian
TP045C	October (Olenya)-16	3990–4030	58.59112	68.32420	Lower Devonian
TP046C	Syurkharatinsk-1	3192–3208	57.77035	67.98129	Upper Devonian
TP047C	Khylchuyu-52	1685–1692	55.29555	68.30529	Upper Permian
TP048C	Yareyu-43	2010–2016	55.45810	67.93231	Lower Permian
TP049C	East Khoreyver-11	2110–2115	58.60032	68.30103	Upper Permian
TP050C	North Sorokinsk-114	1302–1310	58.22574	68.76288	Lower Triassic
TP051C	Tyulysey-80	2018–2026	58.69944	68.37567	Upper Permian
TP052C	Tedinsk-40	3243–3248	57.89806	67.86977	Upper Devonian
TP053C	Pyusey-21	3188–3231	57.93258	67.98156	Upper Devonian
TP054C	Tyulysey-80	2250–2554	58.69944	68.37567	Lower Permian
TP055C	Pechora-Kozhva-103	3021–3242	57.11251	65.20944	Middle Devonian
TP056C	West Sopless-9	4351–4383	57.50888	64.50297	Middle Devonian
TP057C	West Tebuk-300	1892–2006	54.93075	63.64635	Middle Devonian
TP058C	Upper Grubeshor-1	3790–3830	54.89258	66.92322	Middle Devonian
TP059C	Upper Grubeshor-2	3670–3750	54.95046	66.90263	Upper Devonian
TP060C	West Tebuk-300		54.93075	63.64635	Upper Devonian
TP061C	South Nizevaya-4	3817	52.63633	65.46016	Upper Devonian
TP062C	South Yuryakha-15	3268–3272	55.02036	66.71165	Upper Devonian
TP063C	Veyakoshor-5	2147–3211	58.10598	66.82554	Middle–Upper Carboniferous
TP064C	Vuktyl-53	3396–3420	57.46939	63.97357	Middle Carboniferous
TP065C	Layavozh-39	2416–2435	55.10119	67.59817	Upper Carboniferous
TP066C	Upper Vozey-204	3520–3558	57.15312	66.72179	Lower Silurian
TP067C	Taliy-Yu-31		55.71929	64.67268	
TP068C	Makaryel-90	2292–2294.6	53.22950	65.53304	Upper Devonian
TP069C	Makaryel-90	1300	53.22950	65.53304	Upper Devonian
TP070C	Middle Kharyaga-141	3475–3483	56.37138	67.40213	Upper Devonian
TP071C	Lydushor-300	3000–3020	57.40635	67.03307	Upper Devonian
TP072C	Sandivey-122	2281–2290	58.37984	67.01488	Upper Carboniferous
TP073C	Upper Vozey-208	3547–3550	57.07610	66.75467	Lower Silurian
TP074C	Subor-2	3490–3500	58.27720	65.78024	Upper Devonian
TP075C	Makaryel-1	2295–2299	53.23980	65.50996	Upper Devonian
TP076C	Cherpayu-23	2030–2050	60.45371	67.48541	Upper Devonian
TP077C	Cherpayu-23	2100–2128	60.45371	67.48541	Lower Devonian

APPENDIX 2: Continued

Sample Identification	Well Name and Number	Depth (m)	Longitude (North)	Latitude (East)	Reservoir Age
TP078C	Makaryel-90	2280–2294	53.22950	65.53304	Upper Devonian
TP079C	West Aressk-34	784–789	54.80746	64.40816	Upper Permian
TP080C	Makaryel-90	1500	53.22950	65.53304	Upper Devonian
TP081C	South Lyzha-15	2477–2486	56.43438	65.32285	Upper Devonian
TP082C	Yarega-(mine)	30	53.59143	63.39803	Middle Devonian
TP083C	Upper Vozey-202	3324–3352	56.98509	66.73209	Lower Silurian
TP084C	South Yuryakha-16	2654–2660	55.03980	66.69494	Lower Carboniferous
TP085C	Nyadeyu-5	3198–3204	60.49424	67.87837	Lower Devonian
TP086C	Varknava-10	4098–4109	57.84106	68.65706	Upper Silurian
TP087C	Osovey-48	3635–3645	59.95449	67.61267	Upper Silurian
TP088C	Upper Laya-500	4898–4900	55.34719	67.37802	Lower Silurian
TP089C	Upper Laya-500	4490–4496	55.34719	67.37802	Lower Devonian
TP090C	Osovey-48	3492–3508	59.95449	67.61267	Lower Devonian
TP091C	Varknava-11	4052–4077	57.93969	68.62238	Lower Devonian
TP092C	Myadsey-46	3916–3927	59.27673	68.80564	Lower Devonian
TP093C	Inzyrey-206	4681–4685	56.52969	67.53114	Lower Devonian
TP094C	Toboy-14	4033–4066	58.92983	68.89222	Lower Devonian
TP095C	Naulsk-40	4050–4092	58.69068	68.52783	Lower Devonian
TP096C	West Lekkeyaga-47	2665–2672	60.28514	68.27776	Middle Devonian
TP097C	Inzyrey-206	4206–4249	56.52969	67.53114	Upper Devonian
TP098C	Toboy-36	2640–2710	59.09906	68.84575	Upper Devonian
TP099C	West Yareyyaga-1	3772–3796	59.51607	67.73271	Upper Devonian
TP100C	Visovaya-5	3129–3153	58.89120	67.94725	Upper Devonian
TP101C	Medynsk-3	2837–2882	58.84478	68.94370	Upper Devonian
TP102C	Ardalinsk-46	3280–3312	57.24941	67.57958	Upper Devonian
TP103C	North Khosedayu-14	2939–2943	58.91346	67.82030	Upper Devonian
TP104C	Varknava-1	3608–3699	57.94227	68.65517	Upper Devonian
TP105C	Labogan-75	2326–2350	59.01020	68.37003	Lower Carboniferous
TP106C	Upper Kharitseysk-75	2539–2547	62.54023	67.72109	Upper Carboniferous
TP107C	Khylchuyu-16	1932–1937	55.29173	68.33921	Lower Permian
TP108C	South Toravey-35	1362–1377	58.56351	68.58633	Upper Permian
TP109C	North Sorokinsk-106	1123–1137	58.41117	68.65220	Lower Triassic
TP110C	Khylchuyu-52	1643–1663	55.29555	68.30529	Lower Triassic
TP111C	Pyzhyel-5	2494–2499	57.98140	65.72916	Upper Permian
TP112C	Ardalinsk-46	3364.5–3380	57.24941	67.57958	Upper Devonian
TP113C	Dyusyushevsk-58	3308–3324	57.24667	67.45250	Upper Devonian
TP114C	North Kharyaga-6	2131–2135	56.28409	67.51576	Lower Permian
TP115C	North Khosedayu-2	2946–2997	58.84626	67.85303	Upper Devonian
TP116C	West Khosedayu-41	3116–3120	58.24916	67.79011	Upper Devonian
TP117C	Khosolta-91	3657–3665	60.12390	67.39624	Lower Devonian
TP118C	Khosolta-91	3721–3726	60.12390	67.39624	Silurian
TP119C	Sykhorey-1	3090–3104	57.92465	67.74976	Upper Devonian
TP120C	Central Khoreyver-2	3104–3139	57.90910	67.70287	Upper Devonian
TP121C	Khylchuyu-12	2249–2254	55.32102	68.21563	Lower Permian
TP122C	Khylchuyu-20	1664–1685	55.28302	68.27406	Upper Permian
TP123C	South Khylchuyu-21	2218–2237	55.30566	68.18266	Lower Permian
TP124C	South Khylchuyu-24	2255–2262	55.37922	68.20630	Lower Permian
TP125C	Kolguev-123	1900–1910	48.90807	69.25275	Lower Triassic
TP126C	Upper Kolva-60	3169–3190	58.36553	67.99287	Upper Devonian
TP127C	Upper Kolva-65	3195–3200	58.38129	68.00552	Upper Devonian
TP128C	West Lekkeyaga-47	3047–3050; 3054–3070	60.28514	68.27776	Lower Devonian
TP129C	Naulsk-51	1240–1250	58.84382	68.44652	Upper Permian
TP130C	Naulsk-59	1197–1205	58.76422	68.48326	Lower Triassic
TP131C	October (Olenya)-10	4015–4022; 4032–4036	58.18242	68.37106	Lower Devonian
TP132C	October (Olenya)-39	4024–4027	58.38610	68.34740	Lower Devonian
TP133C	October (Olenya)-47	3996–4024	58.66200	68.32282	Lower Devonian

APPENDIX 2: Continued

Sample Identification	Well Name and Number	Depth (m)	Longitude (North)	Latitude (East)	Reservoir Age
TP134C	Ardalinsk-46	3280–3312	57.24941	67.57958	Upper Devonian
TP135C	Passedsk-1	3743–3749	58.24999	68.55379	Upper Devonian
TP136C	Peschanoozersk-4	2872.4–2876	50.07611	69.17316	Upper Carboniferous
TP137C	Peschanoozersk-17	1539–1547	50.01332	69.20262	Lower Triassic
TP138C	North Saremboy-16	3021–3058	60.68076	68.30350	Lower Devonian
TP139C	Sedyaga-10	1000–1022	59.40939	68.14476	
TP140C	North Sykhorey-20	3158–3181	58.03046	67.87289	Upper Devonian
TP141C	North Sykhorey-20	3220–3248	58.03046	67.87289	Upper Devonian
TP142C	North Sorokinsk-113	1344–1349	58.16086	68.82501	
TP143C	Syurkharatinsk-1	3162–3236	57.77035	67.98129	
TP144C	Syurkharatinsk-2	3259–3277	57.71366	67.99746	Upper Devonian
TP145C	Tedinsk-42	3188–3219	57.88465	67.89139	Upper Devonian
TP146C	Toboy-35	2673–2740	59.02844	68.84135	Devonian
TP147C	Toravey-21	1642–1652	58.39851	68.68742	Upper Carboniferous
TP148C	South Toravey-33	1559–1573	58.52987	68.60821	Lower Permian
TP149C	Varknava-9	3677–3696	57.94459	68.68885	Upper Devonian
TP150C	Varknava-9	4029–4083	57.94459	68.68885	Lower Devonian
TP151C	Varandey-2	4294–4322	58.13404	68.83675	Lower Devonian
TP152C	Varandey-4	1630–1677	58.19912	68.78031	Lower Permian
TP153C	Varandey-7	4488–4540	58.13923	68.80930	Silurian
TP154C	Varandey-8	1275	58.11924	68.80057	Lower Triassic
TP155C	Varknava-1	4087–4106	57.94227	68.65517	Lower Devonian
TP156C	East Vasilkovo-71	2457–2539	54.18927	68.11011	Upper Carboniferous
TP157C	Visovaya-6	3182–3211	59.14190	68.00010	Upper Devonian
TP158C	North Yareyyu-150	2265–2330	55.75071	68.09378	Lower Permian

REFERENCES CITED

Abrams, M. A., A. M. Apanel, O. M. Timoshenko, and N. N. Kosenkova, 1999, Oil families and their potential sources in the northeastern Timan-Pechora basin, Russia: AAPG Bulletin, v. 83, no. 4, p. 553–577.

Chalansonnet, S., C. Largeu, E. Casadavall, C. Berkaloff, G. Peniguel, and R. Couderc, 1988, Cyanobacterial resistant biopolymers: Geochemical implications of the properties of *Shizothrix* sp. resistant material: Organic Geochemistry, v. 13, p. 1003–1010.

Collister, J. W., R. E. Summons, E. Lichtfouse, and J. M. Hayes, 1992, An isotopic biogeochemical study of the Green River oil shale (Piceance Creek basin, Colorado): Organic Geochemistry, v. 19, p. 645–659.

Collister, J. W., E. Lichtfouse, G. Hieshima, and J. M. Hayes, 1994, Partial resolution of sources of n-alkanes in the saline poriton of the Parachute Creek Member, Green River Formation (Piceance Creek basin, Colorado): Organic Geochemistry, v. 21, p. 645–659.

de Leeuw, J. W., and C. Largeau, 1993, A review of macromolecular organic compounds that comprise living organisms and their role in kerogen, coal and petroleum formation, *in* M. H. Engel and S. A. Macko, eds., Organic geochemistry: Principles and applications: New York, Plenum Publishing Company, 461 p.

Derenne, S., C. Largeau, E. Casadevall, E. W. Tegelar, and J. W. de Leeuw, 1990, Characterization of Estonian kukersite by spectroscopy and pyrolysis: Evidence for abundant alkyl phenolic moieties in an Ordovician, marine, type II/I kerogen, *in* B. Durand and F. Behar, eds., Advances in organic geochemistry, 1989: Oxford, Pergamon Press, p. 873–888.

Derenne, S., C. Largeau, E. Casadevall, C. Berkaloff, and B. Rousseau, 1991, Chemical evidence of kerogen formation in source rocks and oil shales via selective preservation of thin resistant outer walls of microalgae: Origin of ultralaminae: Geochimica et Cosmochimica Acta, v. 55, p. 1041–1050.

Derenne, S., P. Metzger, C. Largeau, P. F. van Bergen, J.-P. Gatellier, J. S. Sinninghe-Damsté, J. W. de Leeuw, and C. Berkaloff, 1992, Similar morphological and chemical variations of *Gloeocapsomorpha prisca* in Ordovician sediments and cultured *Botryococcus braunii* as a response to changes in salinity, *in* C. B. Eckhard, J. R. Maxwell, S. R. Larter, and D. A. C. Manning, eds., Advances in organic geochemistry 1991: Organic Geochemistry, v. 19, p. 299–231.

Douglas, A. G., J. S. Sinninghe-Damsté, M. G. Fowler, T. I. Eglinton, and J. W. de Leeuw, 1991, Unique distribution of hydrocarbons and sulphur compounds revealed by flash pyrolysis from the fossilised alga *Gloeocapsomorpha prisca*, a major constituent in or of four Ordovician kerogens: Geochimica et Cosmochimica Acta, v. 55, p. 1–17.

Eglinton, T. I., 1994, Carbon isotopic evidence for the origin of macromolecular aliphatic structures in kerogen: Organic Geochemistry, v. 21, p. 721–735.

Fowler, M. G., and A. G. Douglas, 1984, Distribution and structure of hydrocarbons in four organic Ordovician rocks: Organic Geochemistry, v. 6, p. 105–114.

Fowler, M. G., and A. G. Douglas, 1987, Saturated hydrocarbon biomarkers in oils of late Precambrian age from eastern Siberia: Organic Geochemistry, v. 11, p. 201–213.

Full, W. E., R. Ehrlich, and J. C. Bezdek, 1982, Fuzzy QModel— A new approach for linear unmixing: Journal of Mathematical Geology, v. 14, p. 259–270.

Garcette-Lapecq, A., S. Derenne, C. Largeau, I. Bouloubassi, and A. Saliot, 2000, Origin and formation pathways of kerogen-like

organic matter in recent sediments off the Danube delta (northwestern Black Sea): Organic Geochemistry, v. 31, p. 1663–1683.

Gelin, F., J. K. Volkman, C. Largeau, S. Derenne, J. S. Sinninghe-Damsté, and J. W. de Leeuw, 1999, Distribution of aliphatic, nonhydrolyzable biopolymers in marine microalgae: Organic Geochemistry, v. 30, p. 147–159.

Gelpi, E., J. Oro, H. J. Schneider, and E. O. Bennet, 1970, Hydrocarbons of geochemical significance in microscopic algae: Phytochemistry, v. 9, p. 603–612.

Han, J., and M. Calvin, 1969, Hydrocarbon distribution of algae and bacteria and microbiological activity in sediments: Proceedings of the National Academy of Science, v. 64, p. 436–443.

Han, J., E. D. McCarthy, M. Calvin, and M. H. Benn, 1968, Hydrocarbon constituents of the blue-green algae. *Nostoc muscorum*, *Anacyctis nidulans*, *Phormidium luridum* and *Chlorogloea fritschii*: Journal of the Chemical Society, section C, p. 2785–2791.

Han, J., E. D. McCarthy, W. VanHoeven, and W. H. Bradley, 1980, Organic geochemical studies II. A preliminary report on the distribution of aliphatic hydrocarbons in algae, bacteria and a recent lake sediment: Proceedings of the National Academy of Science, v. 59, p. 29–33.

Hatch, J. R., S. R. Jacobson, B. J. Witzke, J. B. Risatti, P. E. Anders, E. L. Watney, K. D. Newell, and A. K. Vuletich, 1987, Possible late Mid-Ordovician organic hydrocarbon source rocks, mid-continent and east-central United States: AAPG Bulletin, v. 71, p. 1342–1354.

Johnson, G. W., R. Ehrlich, and W. Full, 2002, Principal components analysis and receptor models environmental forensics, *in* B. L. Murphy and R. D. Morrison, eds., Introduction to environmental forensics: New York, Academic Press, p. 461–515.

Jones, J. G., 1969, Studies on lipids of soil microorganisms with particular reference to hydrocarbons: Journal of General Microbiology, v. 59, p. 145–152.

Jones, J. G., and B. V. Young, 1970, Major paraffin constituents of microbial cells with particular reference to *Chromatium* sp.: Archive fur Mikrobiologie, v. 70, p. 82.

Largeau, C., S. Derenne, C. Clairay, E. Casadevall, J. F. Raynaud, and N. Sellier, 1990, Characterization of various kerogens by scanning electron microscopy (SEM) and transmission electron microscopy (TEM)— Morphological relationships with resistant outer walls in extant microorganisms: Mededelingen Geology Dienst, v. 45, p. 91–101.

Mackenzie, A. S., S. C. Brassell, G. Eglinton, and J. R. Maxwell, 1982, Chemical fossils: The geological fate of steroids: Science, v. 217, p. 223–226.

Metzger, P., C. Largeau, and E. Casadevall, 1991, Lipids and macromolecular lipids of the hydrogen-rich microalga *Botryococcus braunii*. Chemical structure and biosynthesis-geochemical biotechnological importance, *in* W. Hertz, G. W. Kirby, R. E. Moore, W. Steglich, and C. Tamm, eds., Progress in the chemistry of organic natural products: Paris, Springer-Verlag, v. 57, p. 1–70.

Peters, K. E., and J. M. Moldowan, 1993, The biomarker guide: Interpreting molecular fossils in petroleum and ancient sediments: Englewood Cliffs, New Jersey, Prentice Hall, 363 p.

Peters, K. E., J. W. Snedden, A. Sulaeman, J. F. Sarg, and R. J. Enrico, 2000, A new geochemical-sequence stratigraphic model for the Mahakam delta and Makassar slope, Kalimantan, Indonesia: AAPG Bulletin, v. 84, p. 12–44.

Reed, J. D., H. A. Illich, and B. Horsfield, 1986, Biochemical evolutionary significance of Ordovician oils and their sources, *in* D. Leythaeuser and J. Rullkötter, eds., Advances in organic geochemistry 1985: Oxford, Pergamon Press, p. 347–358.

Requejo, R. G., R. Sassen, M. C. Kennicutt, II, I. Kvedchuk, T. McDonald, G. Denoux, P. Comet, and J. M. Brooks, 1995, Geochemistry of oils from the northern Timan-Pechora basin, Russia: Organic Geochemistry, v. 23, no. 3, p. 205–222.

Ruble, T. E., A. J. Bakel, and R. P. Philp, 1994, Compound specific isotopic variability in Uinta basin native bitumens: Paleoenvironmental implications: Organic Geochemistry, v. 21, p. 661–671.

Shanmugam, G., 1985, Significance of coniferous rainforests and related organic matter in generating commercial quantities of oil, Gippsland basin, Australia: AAPG Bulletin, v. 69, p. 1241–1254.

Shiea, J., S. C. Brassell, and D. M. Ward, 1990, Mid-chain branched mono- and dimethyl alkanes in hot spring cyanobacterial mats: A direct biogenic source for branched alkanes in ancient sediments?: Organic Geochemistry, v. 15, p. 223–231.

Stasiuk, L. D., B. D. Kybett, and S. L. Bend, 1993, Reflected light microscopy and micro-FTIR of Upper Ordovician *Gloeocapsomorpha prisca* alginite in relation to paleoenvironment and petroleum generation, Saskatchewan, Canada: Organic Geochemistry, v. 20, p. 707–719.

Summons, R. E., and M. R. Walter, 1990, Molecular fossils and microfossils of prokaryotes and protists from Proterozoic sediments: American Journal of Science, v. 290-A, p. 212–244.

Tegelaar, E. A., J. W. de Leeuw, S. Derenne, and C. Largeau, 1989, A reappraisal of kerogen formation: Geochemica et Cosmochimica Acta, v. 53, p. 3103–3106.

Tull, S. J., 1997, The diversity of hydrocarbon habitat in Russia: Petroleum Geoscience, v. 3, p. 315–325.

Tyson, R. V., 1995, Sedimentary organic matter: New York, Chapman and Hall, 615 p.

Ulmischek, G., 1982, Petroleum geology and resource assessment of the Timan-Pechora basin, U.S.S.R. and the adjacent Barents–northern Kara shelf: Argonne National Laboratory Report, ANL/EES-TM-199, 197 p.